

AD-A066 085

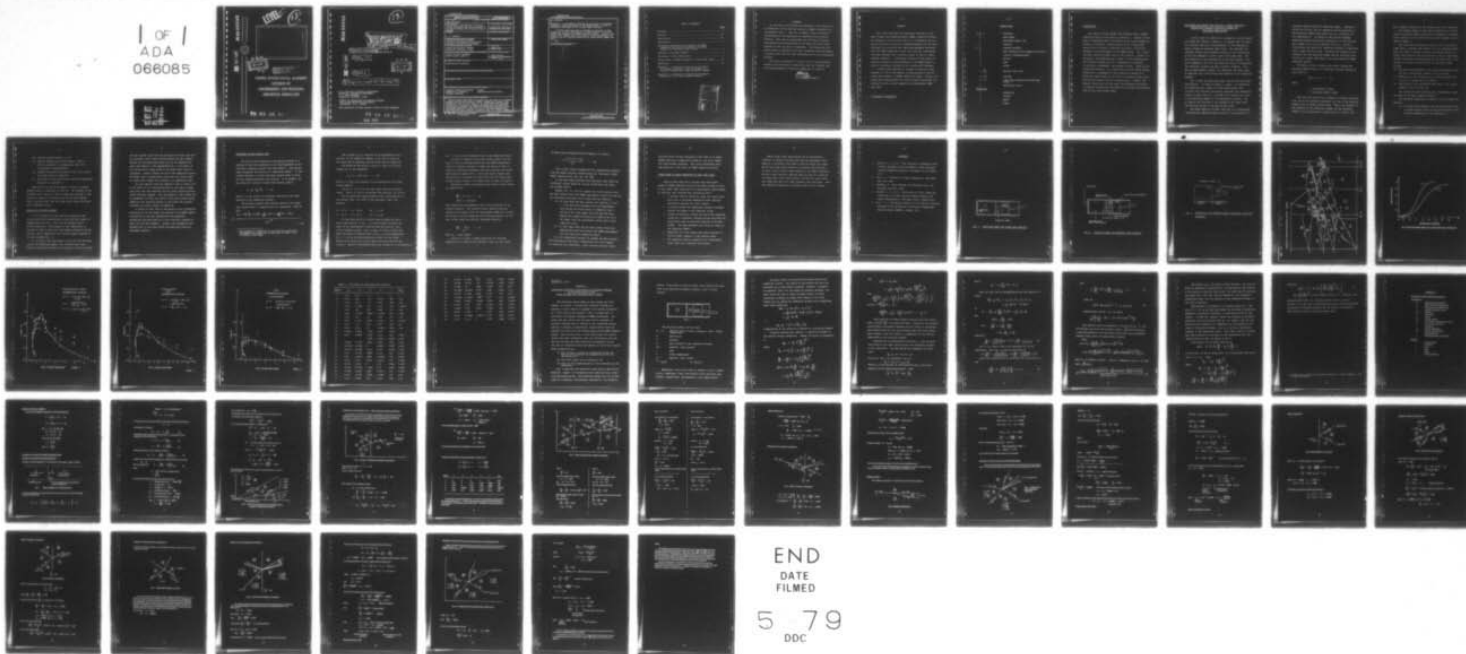
NAVAL ACADEMY ANNAPOLIS MD DIV OF ENGINEERING AND WEAPONS F/G 21/2  
PRELIMINARY INVESTIGATION OF THE NONSTEADY COMBUSTION AND FLOW --ETC(U)  
MAY 78 R P PANDALAI, A A POURING

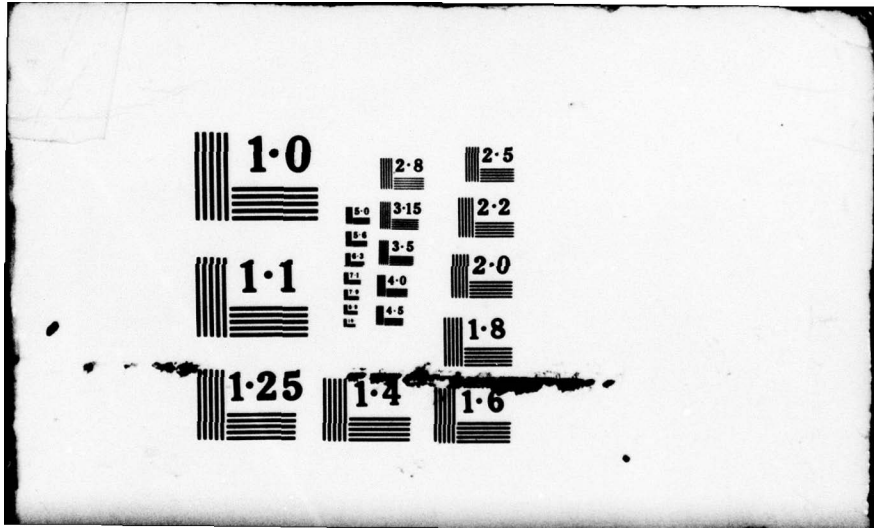
UNCLASSIFIED

USNA-EW-10-78

NL

1 OF 1  
ADA  
066085





1.0

2.8

2.5

3.15  
3.5  
4.0  
4.5

3.15

2.2

1.1

3.5

2.0

4.0

4.5

1.8

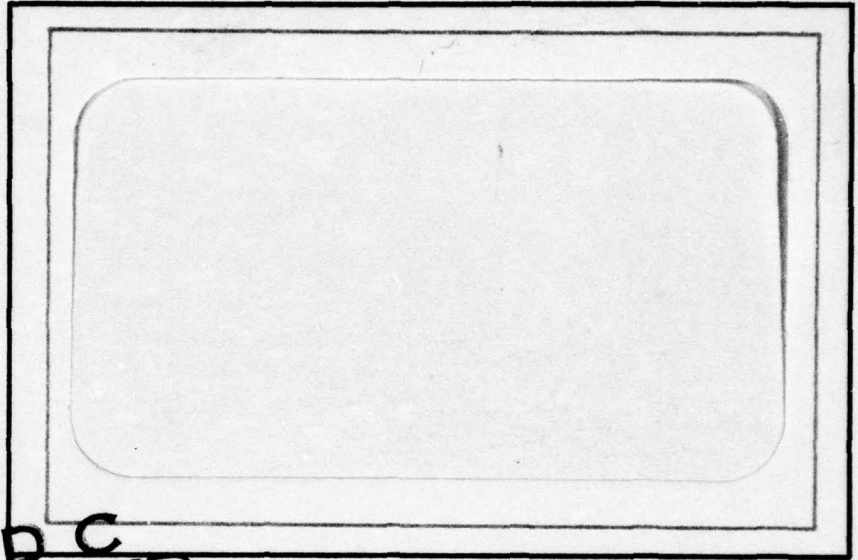
1.25

1.4

1.6

**LEVEL II**

13<sub>B</sub>



**AD A0 66085**

**DDC FILE COPY**



**DDC**  
**RECEIVED**  
MAR 20 1979  
*C*

This document has been approved for public release and sale; its distribution is unlimited.

**UNITED STATES NAVAL ACADEMY  
DIVISION OF  
ENGINEERING AND WEAPONS  
ANNAPOLIS, MARYLAND**

**79 03 16 07**

ADA066085

13

6 PRELIMINARY INVESTIGATION OF THE NONSTEADY COMBUSTION AND FLOW PROCESSES OF THE NAVAL ACADEMY HEAT BALANCED ENGINE (NAHBE)

10 RAGHAVAN P. / PANDALAI A.A. / Pouring

14 USNA-EW-10-78 MAY 1978 REPORT EW-10-78

DDC FILE COPY

11 May 78

12 64 p.

DDC RECEIVED MAR 20 1979

9 Progress Rept. Jul 76 - Sep 77

A. A. Pouring, Principal Investigator  
Aerospace Engineering Department  
U. S. Naval Academy  
Annapolis, Maryland 21402

\*School of Engineering and Applied Science  
The George Washington University  
Washington, D. C. 20052

Work sponsored by Power Branch, Office of Naval Research

79 03 16 074  
406 923

alt

UNCLASSIFIED

SECURITY CLASSIFICATION OF THIS PAGE (When Data Entered)

REPORT DOCUMENTATION PAGE		READ INSTRUCTIONS BEFORE COMPLETING FORM
1. REPORT NUMBER USNA EW-10-78 ✓	2. GOVT ACCESSION NO.	3. RECIPIENT'S CATALOG NUMBER
4. TITLE (and Subtitle) Preliminary Investigation of the Non-steady Combustion and Flow Processes of the Naval Academy Heat Balanced Engine (NAHBE)		5. TYPE OF REPORT & PERIOD COVERED Progress-Jul 76-Sep 77
		6. PERFORMING ORG. REPORT NUMBER
7. AUTHOR(s) R. P. Pandalai		8. CONTRACT OR GRANT NUMBER(s)
9. PERFORMING ORGANIZATION NAME AND ADDRESS United States Naval Academy Division of Engineering and Weapons Aerospace Engineering Department		10. PROGRAM ELEMENT, PROJECT, TASK AREA & WORK UNIT NUMBERS
11. CONTROLLING OFFICE NAME AND ADDRESS United States Naval Academy Annapolis, Maryland 21402		12. REPORT DATE June 1978
		13. NUMBER OF PAGES
14. MONITORING AGENCY NAME & ADDRESS (if different from Controlling Office) Office of Naval Research Power Branch, Code 473		15. SECURITY CLASS. (of this report) Unclassified
		15a. DECLASSIFICATION/DOWNGRADING SCHEDULE N/A
16. DISTRIBUTION STATEMENT (of this Report) Distribution unlimited.		
17. DISTRIBUTION STATEMENT (of the abstract entered in Block 20, if different from Report)		
18. SUPPLEMENTARY NOTES		
19. KEY WORDS (Continue on reverse side if necessary and identify by block number) Internal Combustion Engines      Energy Combustion, nonsteady              Characteristics diagrams Pressure exchange		
20. ABSTRACT (Continue on reverse side if necessary and identify by block number) → This report describes the analytical work done on the Naval Academy Heat Balanced Engine (NAHBE) combustion Process. The purpose of this one year study is to investigate the proposed utilization of pressure exchange mechanism and the basic non-steady flow processes and combustion phenomena associated with the NAHBE combustion system, utilizing the experimental test data obtained over a period of years at the U. S. Naval Academy.		

DD FORM 1473 1 JAN 73

EDITION OF 1 NOV 65 IS OBSOLETE  
S/N 0102-014-6601

UNCLASSIFIED

SECURITY CLASSIFICATION OF THIS PAGE (When Data Entered)

→ 202

UNCLASSIFIED

SECURITY CLASSIFICATION OF THIS PAGE(When Data Entered)

20. (Cont'd)

Annapolis. A preliminary analysis of the effect of pressure exchange on the performance of the NAHBE engine is given in reference (5) based on the 'volume mode' approach.

A 'front mode' approach is assumed to construct a wave diagram as a first step towards an understanding of the non-steady flow dynamics of NAHBE combustion system. Further, two simple heat release models are used to obtain expressions for pressure and the results compared with experimental NAHBE test data.

\*Included as Appendix 1

UNCLASSIFIED

SECURITY CLASSIFICATION OF THIS PAGE(When Data Entered)

TABLE OF CONTENTS

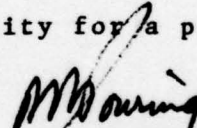
	<u>Page</u>
Foreword .....	1
Abstract .....	ii
Nomenclature .....	iii
Introduction .....	1
Preliminary Non-Steady Flow Analysis of NAHBE Combustion Process with Adiabatic Balancing Chamber and Stationary Power Piston .....	2
Analysis of the Wave Diagram .....	5
Discussion of Heat Release Rate .....	7
Visual Study of NAHBE Combustion at Very Light Loads .....	11
References .....	13
Appendix 1 - Preliminary Analysis of the Effect of Pressure Exchange on the Performance of the Naval Academy Heat Balanced Engine (NAHBE)	
Appendix 2 - Derivation of Equations and Sample Calculations (For Wave Diagram Analysis)	

ACCESSION FOR	
NTIS	Wide Section <input checked="" type="checkbox"/>
DDC	B.II Section <input type="checkbox"/>
UNANNOUNCED	<input type="checkbox"/>
JUSTIFICATION	
BY	
DISTRIBUTION	
Dist.	
A	

FOREWORD

At the time of formulating the statement of the problem to be undertaken in this work the process of NAHBE combustion was as defined in Ref. 1. That is, a general, mostly qualitative understanding of the hypothesis of combustion with pressure exchange. This work was undertaken with the hope of gaining some quantitative understanding of the upper and lower bounds possible in this new mode of combustion. The volume mode and frontal mode of combustion were thus considered with some degree of success even with the crude approximations of this preliminary analysis.

The study is scheduled to continue with a second graduate student at the University of Maryland, since Mr. Pandalai has left George Washington University for a post in industry.

  
A. A. POURING  
Principal Investigator



ABSTRACT

This report describes the analytical work done on the Naval Academy Heat Balanced Engine (NAHBE) Combustion Process. The purpose of this one year study is to investigate the proposed utilization of pressure exchange mechanism and the basic nonsteady flow processes and combustion phenomena associated with the NAHBE combustion system, utilizing the experimental test data obtained over a period of years at the U.S. Naval Academy, Annapolis. A preliminary analysis of the effect of pressure exchange on the performance of the NAHBE engine is given in reference (5)\* based on the "volume mode" approach.

A "front mode" approach is assumed to construct a wave diagram as a first step towards an understanding of the non-steady flow dynamics of NAHBE combustion system. Further, two simple heat release models are used to obtain expressions for pressure and the results compared with experimental NAHBE test data.

---

\* Included as Appendix 1

NOMENCLATURE

A, B, $\alpha$	Constants
M	Mach number
n	Rotational speed, rpm
p	Pressure
P, Q	Riemann variables
Q	Heat released in the combustion process
U	Velocity (nondimensional)
S	Entropy
t	Time
V	Volume
$\gamma = \frac{c_p}{c_v}$	Specific heat ratio
$w = 2\pi n$	Constant
$\theta = \omega t$	Crank angle measured from top dead center
$\phi$	Equivalence ratio
<u>Subscripts</u>	
c	Combustion
o	Initial
s	Shock
t	Total

INTRODUCTION

The nature of Naval Academy Heat Balanced Engine (NAHBE) Combustion System is described in reference 1. Because of the lack of information about the details of the actual combustion process, a preliminary analysis based on the "volume mode" approach was initiated to determine the effect of pressure exchange on the performance of the NAHBE engine. Fig. 1 shows the basic analytical model used in this analysis. Region 1 is occupied by the combustion gas, region 2 by the balancing gas. The interface between the two is simulated by a massless, frictionless, impermeable, and adiabatic piston. Based on the volume mode analysis, it is shown that the  $p(t)$  history during combustion is independent of the presence or absence of a balancing chamber both for the case of stationary power piston and the more general case of a moving piston. Further, the analysis shows that for both cases, the proposed utilization of pressure exchange has the effect of increasing the available work for any given energy input.

PRELIMINARY NON-STEADY FLOW ANALYSIS OF NAHBE COMBUSTION  
PROCESS WITH ADIABATIC BALANCING CHAMBER AND  
STATIONARY POWER PISTON

A "front" mode of combustion is assumed for the preliminary non-steady flow analysis, wherein it is assumed that the chemical reactions take place instantaneously as the unburned gas passes through an advancing flame front. This approach considerably reduces the procedures involved in the construction of the wave diagrams on either side of the flame front. The main objective of the construction of the wave diagram is to get an immediate "feel" for the nature and type of interactions and transients involved and their relative strengths. Also one can approximately compute the combustion time which plays an important role in the nature and formation of the combustion products.

Fig. 2 shows the analytical model used for the non-steady flow analysis. As shown in Figure 1, region 1 is occupied by the combustion gas, region 2 by the balancing gas (Air). Initially the interface which merely separates the combustible mixture of gases from air is assumed to be located very close to the balancing chamber at the beginning of ignition. But as long as the interface is not reached by the flame front, the state of the gas is the same on both sides.

The NAHBE combustion differs from that of a conventional spark ignition combustion mainly because of the presence of a

secondary chamber called the balancing chamber. Reference 1 points out the fact that no combustion has been observed in the balancing chamber which merely acts as a reservoir of hot compressed air. According to the pressure exchange mechanism proposed therein, the balancing air is fed into the main chamber later in the combustion cycle as a result of interactions and thereby the combustion proceeds to completion over a longer period of time. Therefore the movement of the interface into the balancing chamber and the resulting interactions are of great importance to an understanding of NAHBE combustion process.

The plane circular interface once after reaching the balancing chamber moves as a cylindrical interface having an area given by

$$\text{area} = 2\pi rt \quad \text{----} \quad (1)$$

where

r = instantaneous radius

t = balancing chamber length

Note that the area of this cylindrical interface decreases with time as the interface approaches the stem of the balancing chamber prior to being reflected back. Hence, the movement of the interface in the combustion chamber and the balancing chamber can be visualized as taking place in a conical tube

with a gradual reduction in the surface area of the interface.

This gradual change in area can be idealized as a finite number of discrete change in area for the purpose of constructing the details of the interactions on a wave diagram. This is shown in Figure 3.

Once ignition of the mixture occurs at the closed end, a flame front is produced and advances into the unburned mixture. Since the flame is assumed to reach its burning velocity instantly upon ignition, the acceleration of the gas takes place through a shock wave traveling ahead of the flame front. This results in a series of interactions and transients which include:

- (1) The shock wave generated at the closed end interacts with the first discontinuous change of cross section.
- (2) Deflection of the interface by the reflected shock wave at the first change of cross section.
- (3) Interaction of the transmitted shock wave at the second change of cross section, etc.

The interactions and transients that subsequently follow are shown in the wave diagram of Figure 4.

The following assumptions are made in the non-steady flow analysis:

- (a) The flame front advances into the unburned gas with a burning velocity that is taken proportional to the absolute temperature of the unburned gas.

- (b) Initial air/fuel ratio =  $\alpha = 20$
- (c) Initial temperature of the mixture =  $1200^\circ \text{R}$   
[This corresponds to a compression ratio of 8 for adiabatic transformation].
- (d) Changes of pressure and specific heat ratio across the flame front are neglected.
- (e) The motion of the power piston during the combustion processes is negligible.

Construction of the wave diagram is based on standard methods given in references (2) and (3). The movement of the interface with respect to time as combustion proceeds to completion is shown by the dotted lines on the wave diagram. After a certain time, when the flame front reaches the interface, combustion stops.

#### ANALYSIS OF THE WAVE DIAGRAM

It is interesting to note that the strength of the initial shock wave characterized by the shock mach number is comparatively low ( $M_s = 1.247$ ) for the assumed typical initial conditions. The progress of the computations is recorded in Table 1 which give the Riemann parameters and the pressure ratios computed for the various regions labelled in the wave diagram (Fig. 4).

It is clearly seen from Figure 4 that once the interface reaches the balancing chamber, the reflected waves from previous interactions moving in the opposite direction towards

the main chamber slows down the interface and after some time the interface itself starts moving towards the main chamber. Because the reflected shock waves are all of comparatively small mach numbers in the neighborhood of 1.1 the effect of the interaction of these waves on the flame front itself is negligible. However towards the end of the combustion process the flame front is appreciably slowed down and finally when the flame front reaches the interface, the combustion stops.

For this specific case the combustion time is found to be of the order of 0.15 millisecond which is one order of magnitude lower than that observed from the actual engine pressure-volume indicator diagram. This discrepancy is most likely due to assumption (e) where the motion of the power piston during combustion was neglected whereas in the actual more general situation this motion cannot be neglected.

It should be noted that in the absence of any information pertaining to the non-steady flow process in the NAHBE engine, construction of the wave diagram with the simplified assumptions mentioned above as a first step give valuable insight into the flow dynamics. Further, the information thus obtained will in turn help refine the analytical model for subsequent analysis.



DISCUSSION OF HEAT RELEASE RATE

The rate of heat release of a burning gas mixture as a function of the flow conditions is very much dependent on the particular combustion process and flow geometry. Burning proceeds throughout the mixture in a complicated manner. It thus becomes necessary to select some heat release model on which the wave diagram procedures can be based. As an example, one may assume for instance a linear heat release, namely,

$$Q = Q_t \left( \frac{t - t_i}{t_c} \right) \text{ ---- (2)}$$

where  $t_i$  is the initial (or ignition) time and  $t_c$  the total duration of the combustion process.\*

The pressure equation thus obtained based on the linear heat release model is repeated here for convenience. Thus we have

$$p = \frac{c_1 c_2 + \frac{\gamma-1}{2} \frac{Q_t}{wt_c} [wt \sqrt{V_t} + \sqrt{\frac{2}{B}} (A-B) \ln (\sqrt{\frac{B}{2}} wt + \sqrt{V_t})]}{(V_t)^{3/2}} \text{ ---- (3)}$$

\* The duration of combustion in the following analytical development for numerical calculations is taken to be 70 degrees crank angle.

The constant  $c_1 c_2$  in equation (3) is determined by the pressure in the combustion chamber at the time of ignition, the total heat of reaction, and the total time of combustion.

The motion of the piston is given in terms of the total Volume,  $V_t$ , by the expression

$$V_t = A - B \cos (wt) \quad \text{---- (4)}$$

where A, B, and w are constants to be evaluated for the given engine geometry.

Now let  $\theta = wt$  (5) be the crank angle from the top dead center. Thus  $p(\theta)$  can be calculated from equations (3) and (4).

For the particular engine geometry under investigation in the present study, the value of the constants A and B are given by

$$A = 27.22 \quad B = 22.05 \quad - 20^\circ \leq \theta \leq 20^\circ$$

$$A = 25.3 \quad B = 20.1 \quad 20^\circ < \theta \leq 90^\circ$$

At high loads the  $p(\theta)$  history during combustion calculated from equation (3) for  $\gamma = 1.5$  give higher pressures compared to the experimentally observed data particularly later in the expansion stroke. This is shown in Figure 6 which also shows the effect of specific heat ratio,  $\gamma$ , on the calculations. For  $\gamma = 1.35$  the calculated pressure differ from the experimental values during the initial phase following ignition only slightly. However, considerable deviation, though not as pronounced as

for  $\gamma = 1.5$ , is still observed later in the combustion cycle.

In order to improve on this heat release model from the point of view of matching theoretical and NAHBE experimental results an attempt was made to change the nature of heat release to a form more compatible with that observed from actual spark ignition engine tests. Data from several engine tests and reported in reference (4) have shown that the actual heat release diagram follow a "S" shaped curve as shown in Figure 5.

Therefore a family of different heat release curves having the general form

$$\frac{dQ}{d\theta} = \alpha f(\theta) \text{ ---- (6)}$$

where  $\alpha = \text{constant}$

were examined and subsequently used in the derivation of the pressure equation. The pressure levels computed from this equation were compared with the experimental NAHBE test results. On the basis of this comparison the following equation for the heat release model was used for subsequent analysis.

$$\frac{dQ}{d\theta} = \frac{\alpha}{V_t^{\gamma-1}} \text{ ---- (7)}$$

Where  $V_t = \text{total Volume.}$

Equation (7) gives a simple expression for pressure (Equation 8) in terms of two constants  $\alpha$  and  $c_1 c_2$  the values

of which can be evaluated from two known  $p(\theta)$  values.

$$p = \frac{(\gamma-1) \alpha \theta + c_1 c_2}{V_t^\gamma} \quad \text{---- (8)}$$

This is most easily accomplished for computational purposes from the engine indicator diagram using two "arbitrary" points namely ignition point and, say,  $30^\circ$  ATDC.

It has been found necessary from experience that these two "arbitrary" points should be located sufficiently well apart for optimum results.

Figures (6), (7), and (8) compare the results based on the two heat release rates with NAHBE experimental results at 1500 rpm. The following conclusions can be drawn from this analysis:

- (1) At high loads the heat release rate equation (7) with  $\gamma = 1.35$  give good agreement with the experimental data during the initial phase of combustion over a period of  $30^\circ$  crank angles from the ignition time. However the computed pressures are found to be 20 to 80% higher than the experimental values later in the combustion cycle.
- (2) At very light loads the two heat release rates give comparatively good correlation with NAHBE experimental data over the entire combustion phase.

It is of considerable interest to compare the above results with experimental data from a conventional otto cycle engine for identical test conditions. Since accurate pressure traces

from the latter are not available at this time it is recommended that such a comparison be made as otto cycle engine test data becomes available. This could conceivably shed some light as to the nature of NAHBE combustion process.

#### VISUAL STUDY OF NAHBE COMBUSTION AT VERY LIGHT LOADS

Direct visual observation through high speed photographs of NAHBE combustion process with ethyl alcohol as fuel at very light loads conducted on an experimental square engine at 1000 rpm. have revealed some interesting facts.

1. A reaction zone of relatively large size and of pale blue color is observed immediately after ignition followed by multiple hot spots (glows).
2. In certain frames the combustion intensity increases towards the middle of the expansion stroke.
3. Glowing of particles towards the end of the expansion stroke and a subsequent sweeping action even while the piston moves down is generally observed in the main chamber. The same phenomena also occurs at times in the balancing chamber.
4. Appearance of a blue region even before ignition in certain frames suggests a long ignition delay.
5. The combustion duration appears to be considerably larger than that originally anticipated.

While these visual observations are of considerable interest, it should be pointed out that the photographs were taken at a relatively slow speed of 200-250 frames per second and at very light loads because of practical considerations. In order to gain further understanding of the NAHBE combustion process a more realistic approach would be that of increasing the frame speed (which helps observe the particle path lines) and conducting some tests under moderate load conditions. Thus the combustion phenomena at different loads can be studied.

REFERENCE

1. Pouring, A. A. et al., "The influence of Combustion with Pressure Exchange on the Performance of Heat Balanced Internal Combustion Engines," SAE paper 770 120, March, 1977.
2. Foa, J. V., "Elements of Flight Propulsion," John Wiley, New York, 1960.
3. Rudinger, G., "Wave Diagrams for Nonsteady Flow," Van Nostrand, New York, 1955.
4. Heywood, J. B. et al., "Predictions of Nitric Oxide Concentrations in a Spark-Ignition Engine Compared with Exhaust Measurements," SAE paper 710011, January 1971.
5. Foa, J. V., "Preliminary Analysis of the Effect of Pressure Exchange on the Performance of the Naval Academy Heat Balanced Engine (NAHBE)," October, 1976.

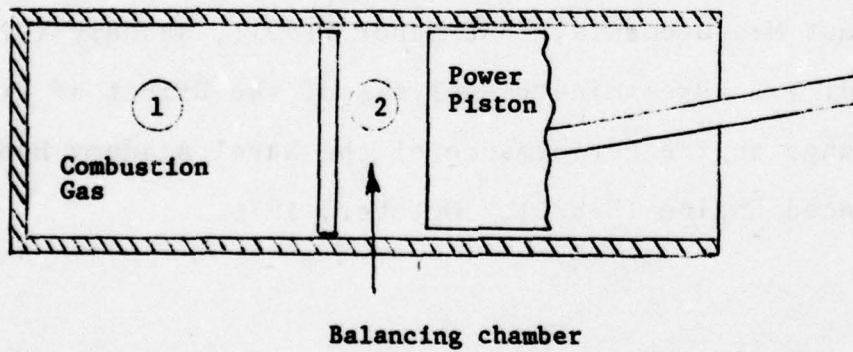


FIG. 1. ANALYTICAL MODEL FOR VOLUME MODE ANALYSIS.



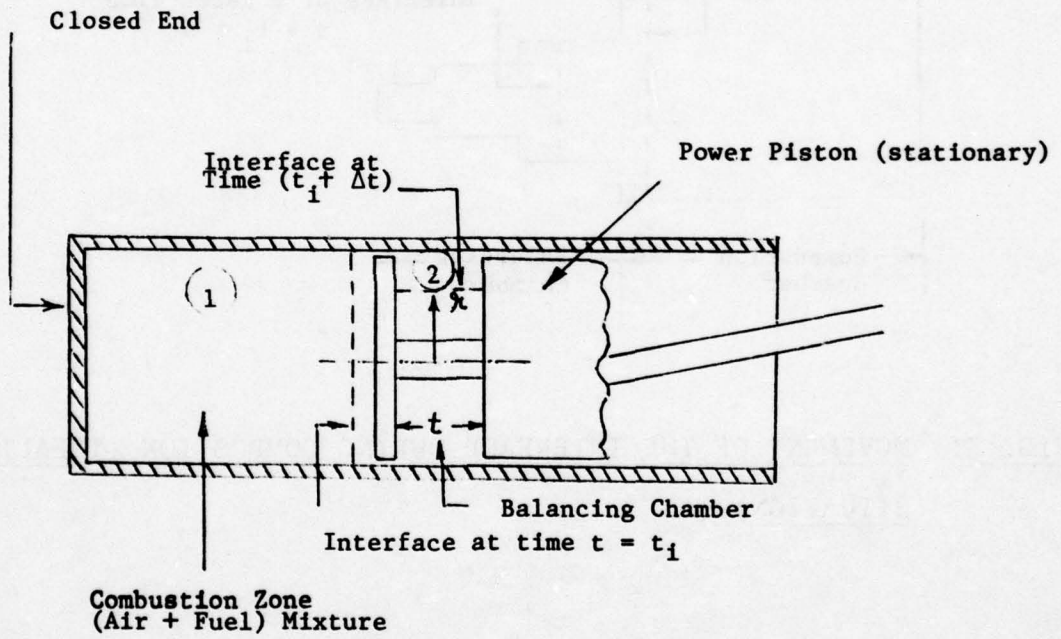


FIG. 2. ANALYTICAL MODEL FOR NONSTEADY FLOW ANALYSIS.

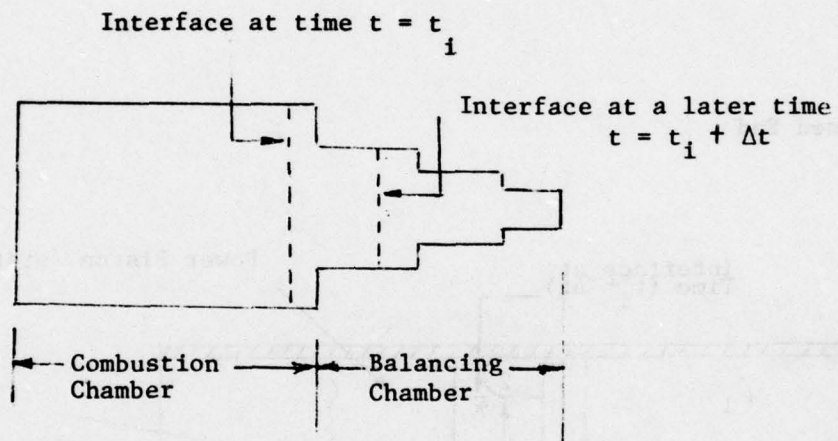
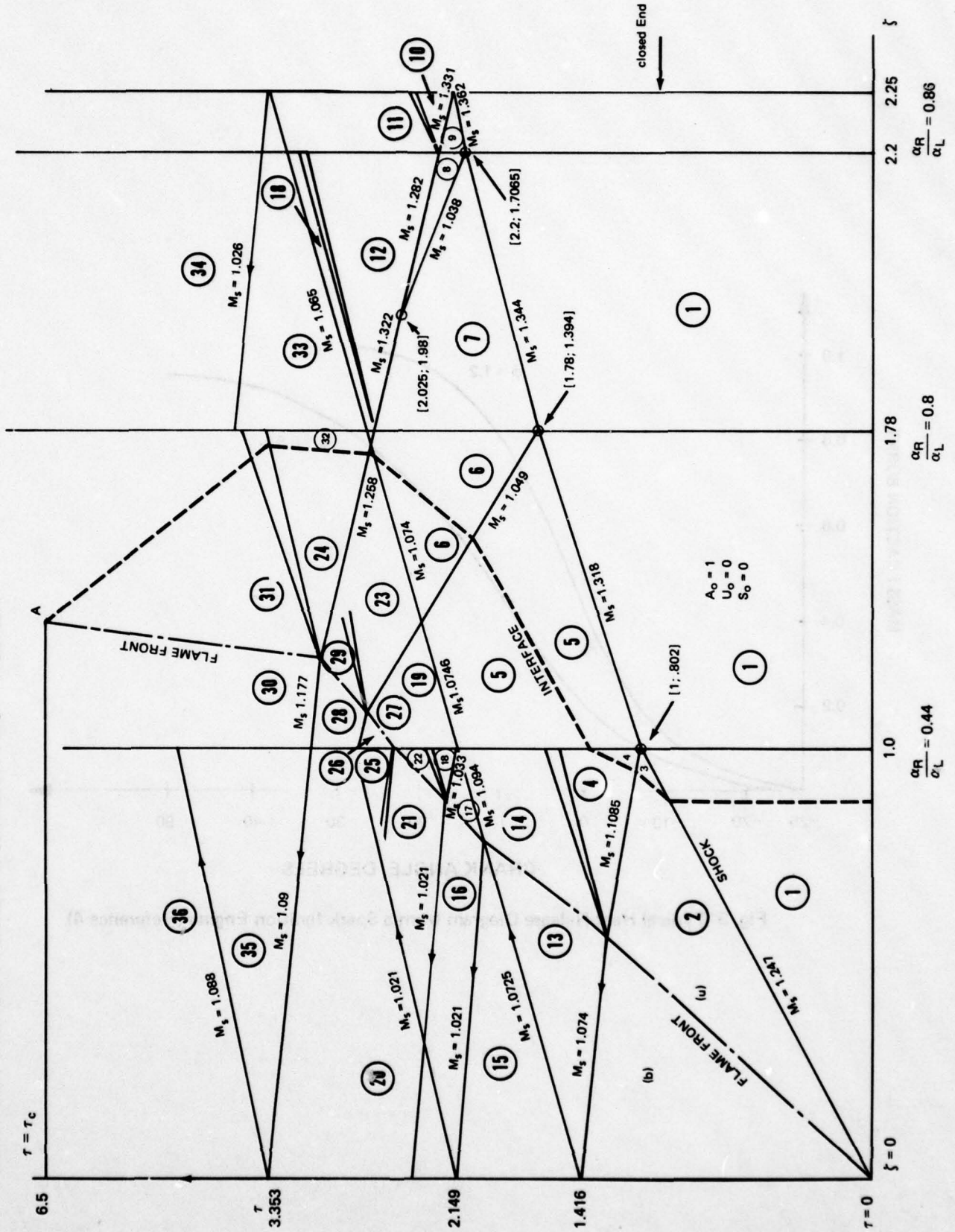


FIG. 3. MOVEMENT OF THE INTERFACE DURING COMBUSTION (IDEALIZED SITUATION).

NONSTEADY FLOW WAVE DIAGRAM (QUALITATIVE) FIGURE 4



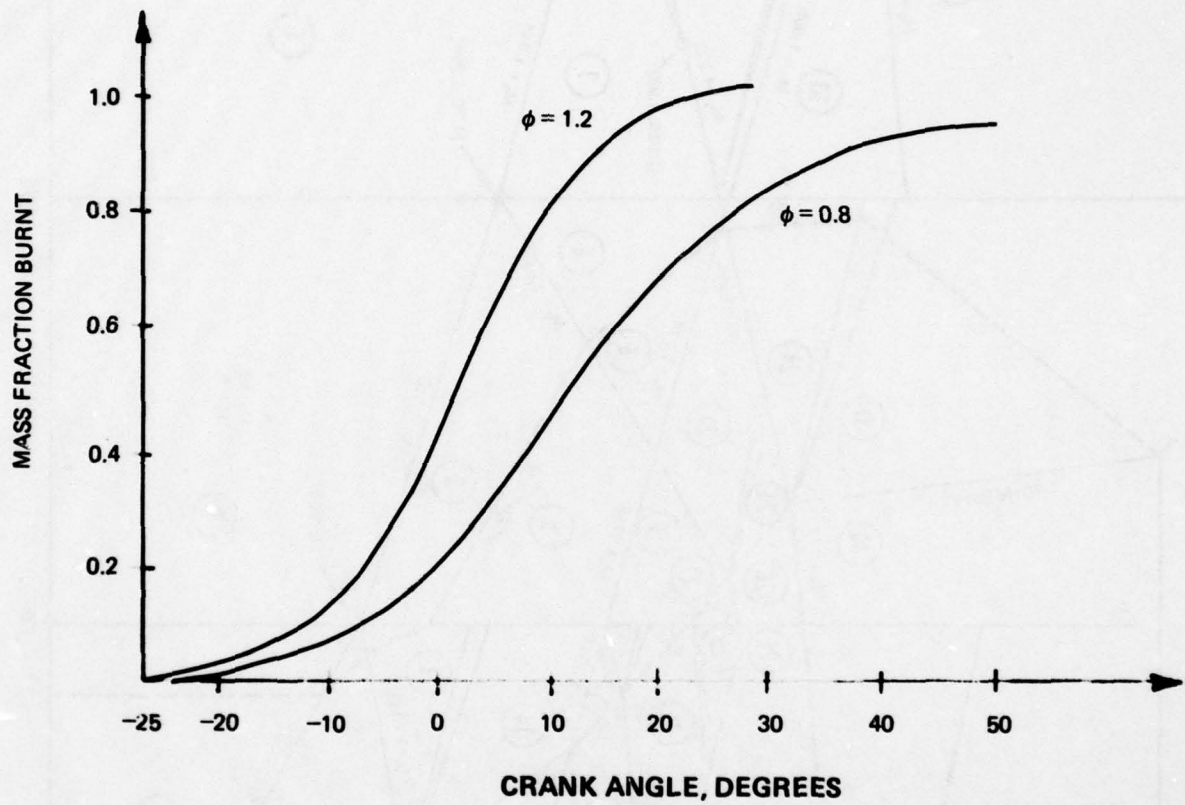


Fig. 5 Typical Heat Release Diagram from a Spark Ignition Engine (Reference 4)

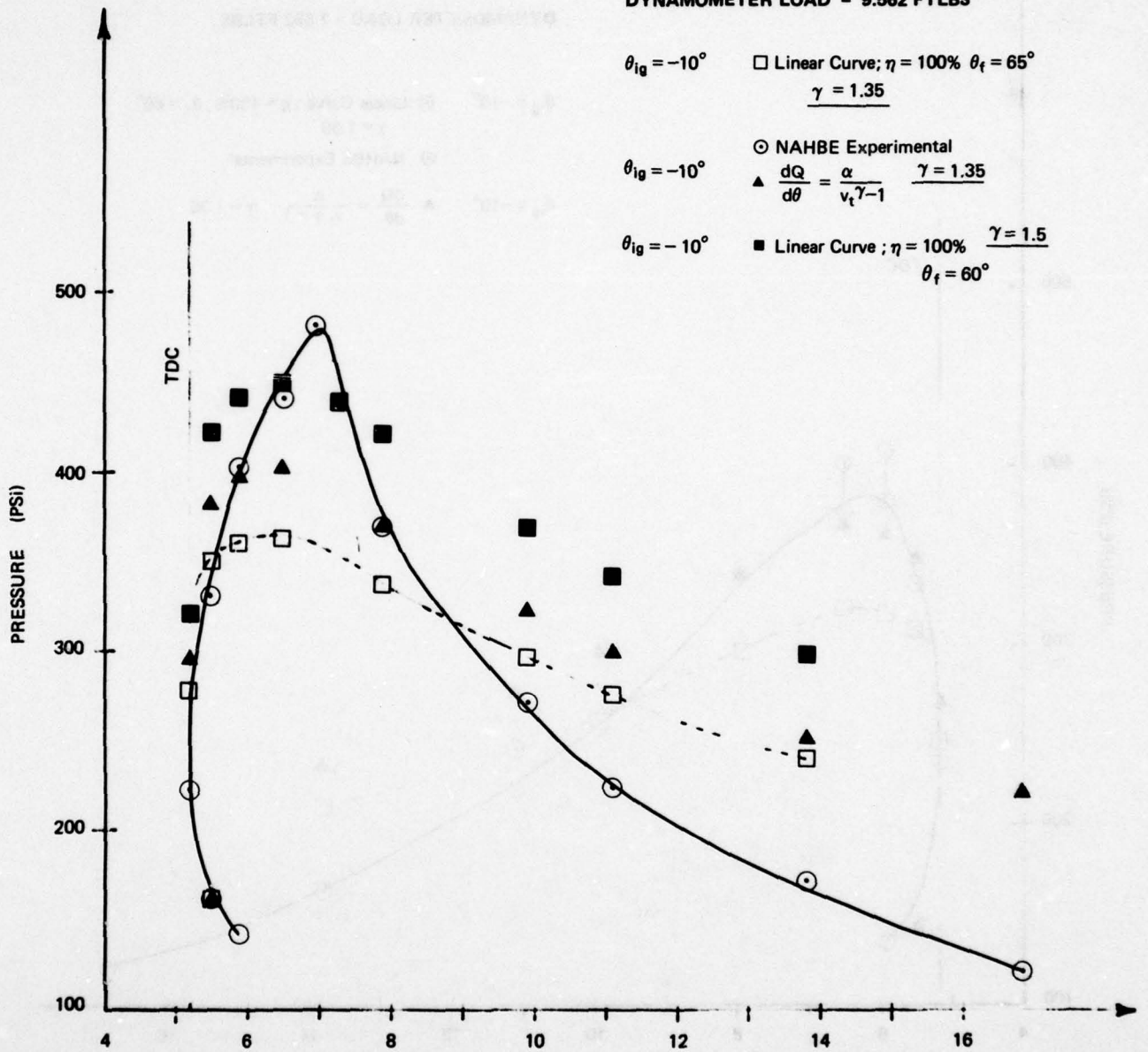
MODE U NOMINAL SPEED = 1500 RPM

DYNAMOMETER LOAD = 9.562 FTLBS

$\theta_{ig} = -10^\circ$      $\square$  Linear Curve;  $\eta = 100\%$   $\theta_f = 65^\circ$   
 $\gamma = 1.35$

$\theta_{ig} = -10^\circ$      $\circ$  NAHBE Experimental  
 $\triangle$   $\frac{dQ}{d\theta} = \frac{\alpha}{v_t \gamma - 1}$   $\gamma = 1.35$

$\theta_{ig} = -10^\circ$      $\blacksquare$  Linear Curve;  $\eta = 100\%$   $\gamma = 1.5$   
 $\theta_f = 60^\circ$



TOTAL VOLUME, CUBIC INCHES

FIGURE 6

Nominal Speed 1500 RPM

MODE R

DYNAMOMETER LOAD = 7.562 FTLBS

$\theta_{ig} = -10^\circ$   $\square$  Linear Curve ;  $\eta = 100\%$  ,  $\theta_f = 60^\circ$   
 $\gamma = 1.35$

$\circ$  NAHBE Experimental

$\theta_{ig} = -10^\circ$   $\blacktriangle$   $\frac{dQ}{d\theta} = \frac{\alpha}{v_t \gamma - 1}$   $\gamma = 1.35$

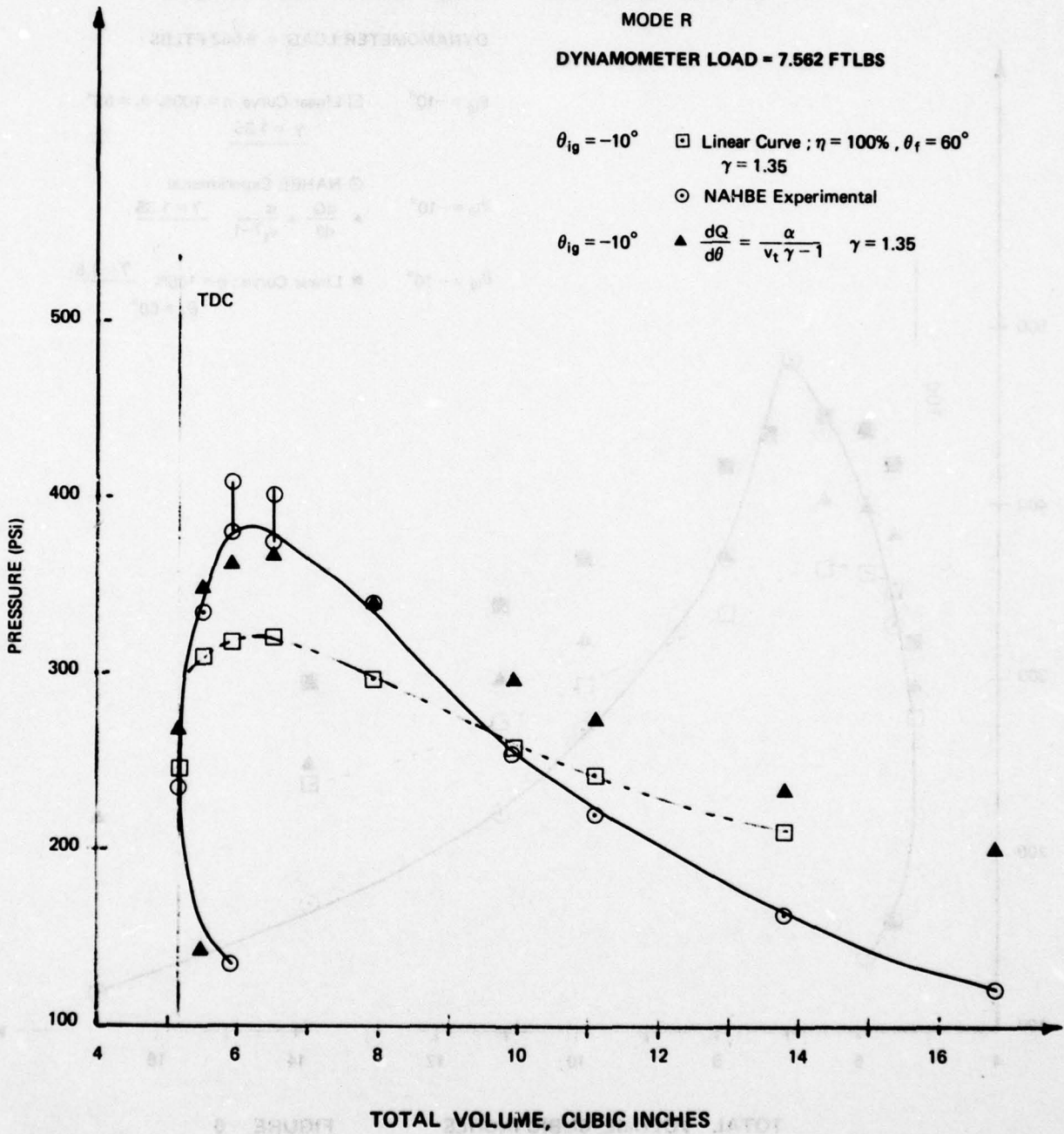


FIGURE - 7

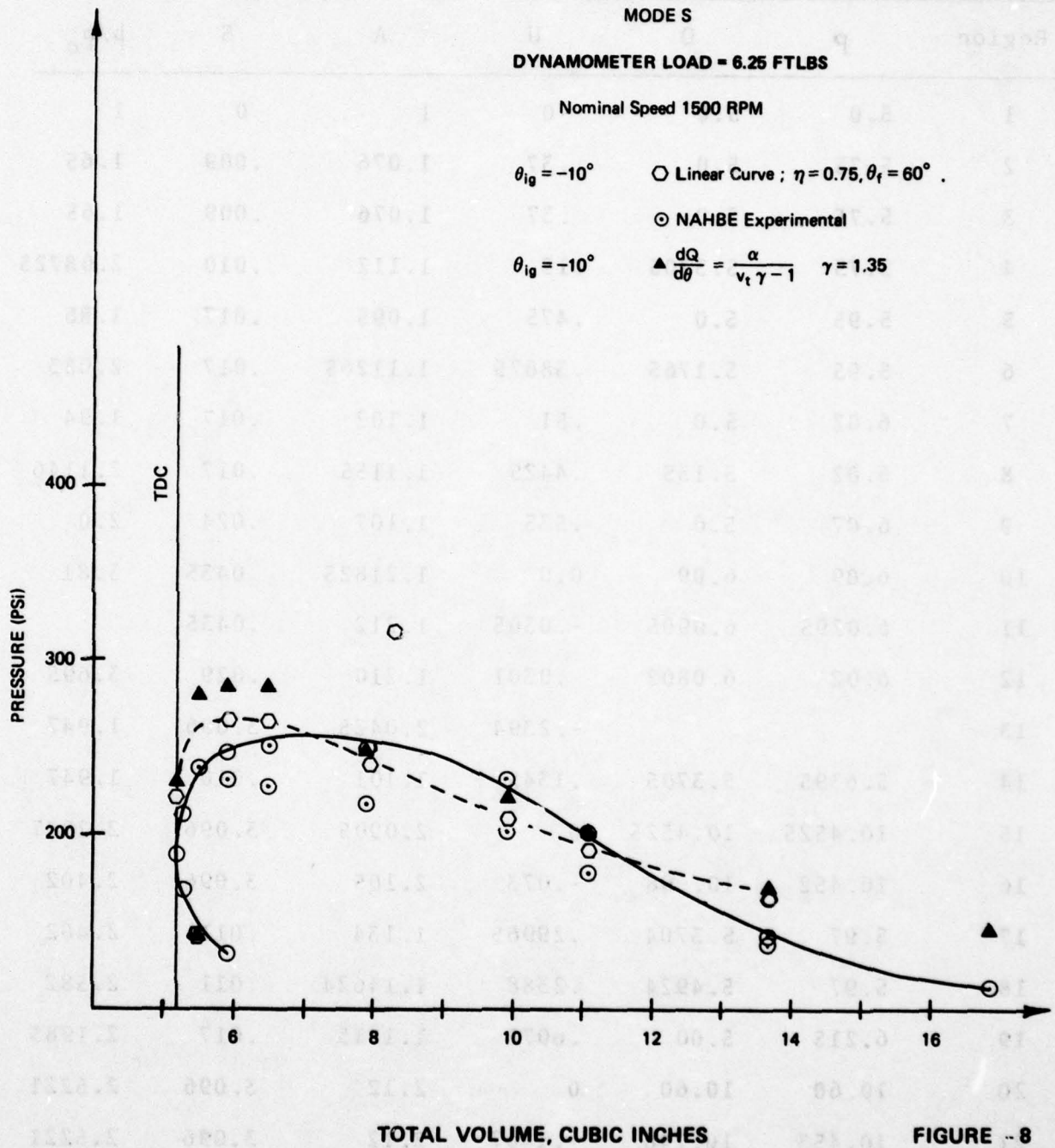


Table 1. Data Sheet for Nonsteady Flow Analysis.

Region	p	Q	U	A	S	p/p <sub>o</sub>
1	5.0	5.0	0	1	0	1
2	5.75	5.0	.37	1.076	.009	1.65
3	5.75	5.0	.37	1.076	.009	1.65
4	5.75	5.3705	.19	1.112	.010	2.08725
5	5.95	5.0	.475	1.095	.017	1.86
6	5.95	5.1765	.38675	1.11265	.017	2.083
7	6.02	5.0	.51	1.102	.017	1.94
8	6.02	5.135	.4425	1.1155	.017	2.1146
9	6.07	5.0	.535	1.107	.024	2.0
10	6.09	6.09	0.0	1.21825	.0435	3.81
11	6.0295	6.0905	-.0305	1.212	.0435	
12	6.02	6.0802	-.0301	1.210	.029	3.695
13			-.2394	2.0425	3.096	1.947
14	5.6395	5.3705	.1345	1.101	.010	1.947
15	10.4525	10.4525	0	2.0905	3.096	2.2877
16	10.452	10.598	-.073	2.105	3.096	2.402
17	5.97	5.3704	.29965	1.134	.011	2.402
18	5.97	5.4924	.2388	1.14624	.011	2.582
19	6.215	5.00	.6075	1.1215	.017	2.1985
20	10.60	10.60	0	2.12	3.096	2.5221
21	10.453	10.746	-.1467	2.12	3.096	2.5221
22	5.9316	5.4924	.2196	1.1424	.011	2.5221
23	6.215	5.1765	.51925	1.13915	.017	2.46
24	6.215	6.069	.073	1.228	.028	4.10



25	10.453	10.297	.078	2.075	3.096	2.169
26	10.546	10.192	.177	2.0738	3.096	2.160
27	6.1869	5.0	.5934	1.1187	.017	2.16
28	10.5483	10.4017	.0733	2.095	3.096	2.31
29	6.1137	5.1763	.4687	1.129	.017	2.31
30	10.5513	11.5487	-.4987	2.21	3.10	3.3495
31	5.8612	6.069	-.1038	1.193	.028	3.3495
32	6.215	6.06	.0775	1.2275	.028	4.088
33	6.1864	6.08	.0532	1.2266	.029	4.0774
34	6.185	6.185	0	1.237	.029	4.322
35	10.60	11.2095	-.30475	2.181	3.097	3.070
36	11.21	11.21	0	2.242	3.098	3.7147

J.V. Foa  
October 15, 1976

Appendix 1

Preliminary Analysis of the Effect of Pressure Exchange  
on the Performance of the  
Naval Academy Heat Balanced Engine (NAHBE)

The relatively large number of wave passes per cycle appears to justify a "volume mode" approach (whereby the pressure at each instant is assumed to be uniform throughout) as a first step in the analysis. What is sought here is the effect of pressure exchange on NAHBE performance. The error that may result from the quasi-static treatment of pressure exchange that is implied in the volume-mode approximation is probably insignificant, because shock waves are unlikely to form within the limited space of the NAHBE chambers anyway. More serious error, on the other hand, will surely result from three assumptions that are dictated here both by the need to make the model analytically manageable and by the lack of information about the details of the actual process.

These assumptions are:

- (1) that no mass or energy is transported across the the interface between the combustion gas and the "balancing gas";
- (2) that flow losses can be neglected, and
- (3) that all the transformations of the balancing gas are isentropic.

Fig. 1 describes the analytical model used in the present analysis. Region 1 is occupied by the combustion gas, region 2 by the balancing gas. The interface between the two is simulated by a massless, frictionless, impermeable, and adiabatic

piston. This piston is free to float, thus allowing the pressure to be equalized throughout regions 1 and 2 at each instant.

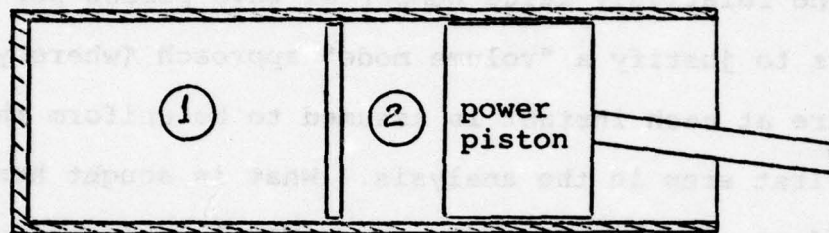


Fig. 1

The following symbols will be used:

$c_p, c_v$	specific heats at const. pressure, const. volume, respectively
$m$	mass of gas
$p$	pressure
$Q$	heat released in the combustion process
$s, S$	specific, total entropy
$t$	time
$T$	static temperature
$v, V$	specific, total volume
$\gamma = c_p/c_v$	$\varphi = v_{i2}/v_{it}$

Subscripts 1 and 2 will refer to regions 1 and 2, respectively; subscripts i and f will denote initial and final conditions, respectively, and subscript t will denote "total".

The power piston will generally be moving during the combustion process. The effect of this motion will be fully accounted for in the present analysis. However, to acquire an immediate "feel" for the effect of pressure exchange, consider first the case in which the power piston is either stationary or moving so slowly that changes of the total volume  $V_t = V_1 + V_2$  during the combustion process can be neglected. Under these conditions,

$$\begin{aligned} dQ &= c_v (m_1 dT_1 + m_2 dT_2) \\ &= \frac{c_v}{R} (p dV_1 + V_1 dp + p dV_2 + V_2 dp) \\ &= \frac{1}{\gamma-1} V_t dp \end{aligned}$$

$\therefore$

$$p_f - p_i = (\gamma-1) Q_t / V_t$$

independently of the presence or absence of a balancing chamber.

Pressure exchange has, however, a significant effect on the overall entropy production. Indeed, by virtue of assumption 3,

$$V_{f2} = V_{i2} \left( \frac{p_i}{p_f} \right)^{1/\gamma}$$

hence

$$V_{f1} = V_t \left[ 1 - \varphi \left( \frac{p_i}{p_f} \right)^{1/\gamma} \right]$$

$$\frac{v_{f1}}{v_{i1}} = \frac{V_{f1}}{V_{i1}} = \frac{1 - \varphi \left( \frac{p_i}{p_f} \right)^{1/\gamma}}{1 - \varphi}$$

$$\begin{aligned} \Delta S_1 &= c_v \ln \frac{p_f}{p_i} + c_p \ln \frac{v_{f1}}{v_{i1}} \\ &= c_p \ln \frac{\left( \frac{p_f}{p_i} \right)^{1/\gamma} - \varphi}{1 - \varphi} \end{aligned}$$

and

$$\Delta S = m_i \Delta s_i$$

$$= \frac{r}{r-1} \frac{p_i V_t}{T_{i1}} (1-\varphi) \ln \frac{\left(\frac{p_t}{p_i}\right)^{1/r} - \varphi}{1-\varphi}$$

Now,

$$\frac{d(\Delta S)}{d\varphi} = \frac{r}{r-1} \frac{p_i V_t}{T_{i1}} \left[ -\ln \frac{\left(\frac{p_t}{p_i}\right)^{1/r} - \varphi}{1-\varphi} + \frac{\left(\frac{p_t}{p_i}\right)^{1/r} - 1}{\left(\frac{p_t}{p_i}\right)^{1/r} - \varphi} \right]$$

Letting  $\frac{\left(\frac{p_t}{p_i}\right)^{1/r} - \varphi}{1-\varphi} = \chi,$

$$\frac{d(\Delta S)}{d\varphi} = \frac{r}{r-1} \frac{p_i V_t}{T_{i1}} \left( -\ln \chi + 1 - \frac{1}{\chi} \right)$$

This quantity is always negative because,  $\chi$  being greater than 1.0,  $\ln \chi = \frac{\chi-1}{\chi} +$  all positive terms. Therefore, the proposed utilization of pressure exchange has the effect of increasing the available work for any given energy input and total volume. Note, however, that this effect is independent of the initial temperature in the balancing chamber.

Consider now the more general situation -- that in which the motion of the power piston during the combustion process is not negligible. Let this motion be a harmonic one, such that

$$V_t = A - B \cos \omega t$$

where A, B, and  $\omega$  are constants, and let

$$Q = Q_t (t - t_i) / t_c$$

where  $t_i$  is the initial (or ignition) time and  $t_c$  the total duration of the combustion process. Then,

$$V_t = A - \cos \epsilon$$

where

$$\xi = \omega \left( \frac{t_c}{Q_t} Q + t_i \right)$$

From the First Law of Thermodynamics and the equation of state,

$$\begin{aligned} dQ - p dV_t &= -c_v (m_1 dT_1 + m_2 dT_2) \\ &= \frac{1}{\gamma-1} (p dV_t + V_t dp) \end{aligned}$$

or

$$\left( 1 - \frac{\gamma}{\gamma-1} p \frac{dV_t}{dQ} \right) dQ = \frac{1}{\gamma-1} V_t dp$$

But

$$dQ = \frac{Q_t}{\omega t_c} d\xi$$

$$\text{and } \frac{dV_t}{dQ} = \omega \frac{t_c}{Q_t} \frac{dV_t}{d\xi}$$

$$= B \omega \frac{t_c}{Q_t} \sin \xi$$

Therefore,

$$\frac{dp}{d\xi} + \frac{\gamma B \sin \xi}{A - B \cos \xi} p = (\gamma-1) \frac{Q_t}{\omega t_c} \frac{1}{A - B \cos \xi} \quad (1)$$

Let  $p = uz$ , where  $u$  and  $z$  are functions of  $\xi$  to be determined. Then, Eq. (1) may be re-written as

$$-u \frac{dz}{d\xi} - \frac{(\gamma-1) Q_t}{\omega t_c (A - B \cos \xi)} = \left( \frac{du}{d\xi} + \frac{\gamma B \sin \xi}{A - B \cos \xi} u \right) z$$

Since this equation must be satisfied for all values of  $z$ ,

set

$$\frac{du}{d\xi} + \frac{\gamma B \sin \xi}{A - B \cos \xi} u = 0 \quad (2)$$

and

$$u \frac{dz}{d\xi} - (r-1) \frac{Q_c}{\omega t_c} \frac{1}{A - B \cos \xi} = 0 \quad (3)$$

From (2),

$$u (A - B \cos \xi)^r = C_1 \text{ (a constant)} \quad (4)$$

Substituting into Eq. (3), we obtain

$$\frac{\omega t_c C_1}{(r-1) Q_c} dz = (A - B \cos \xi)^{r-1} d\xi$$

This equation may be integrated in closed form for  $r = 3/2$  and through the use of the relation  $\cos \xi = 1 - \frac{\xi^2}{2}$ , which provides a good approximation over the range of  $\xi$  within which combustion normally takes place in reciprocating engines.

Then,

$$\begin{aligned} z &= C_2 + \frac{(r-1) Q_c}{\omega t_c C_1} \int [(A-B) + B \frac{\xi^2}{2}]^{1/2} d\xi \\ &= C_2 + \frac{r-1}{2} \frac{Q_c}{\omega t_c C_1} \left[ \xi \sqrt{A-B(1-\frac{\xi^2}{2})} + \sqrt{\frac{2}{B}} (A-B) \ln \left( \xi + \sqrt{\frac{2}{B}} \sqrt{A-B(1-\frac{\xi^2}{2})} \right) \right] \quad (5) \end{aligned}$$

where  $C_2$  is another constant. Finally, remembering that  $p = uz$  and that  $1 - \frac{\xi^2}{2} = \cos \omega t$ ,

$$p = \frac{C_1 C_2 + \frac{r-1}{2} \frac{Q_c}{\omega t_c} \left[ \omega t \sqrt{A-B \cos \omega t} + \sqrt{\frac{2}{B}} (A-B) \ln \left( \omega t + \sqrt{\frac{2}{B}} \sqrt{A-B \cos \omega t} \right) \right]}{\sqrt{A-B \cos \omega t}} \quad (6)$$

The product  $C_1 C_2$  now forms a single constant, the value of which is determined, through Eq. (6), by the position and velocity of the piston at ignition time ( $t=t_i$ ), the total heat of reaction, the engine rpm, the total time of combustion, the volumetric compression ratio, and the pressure in the combustion chamber at the time of ignition.

The average  $\gamma$  in combustion is actually around 4/3. The use of  $\gamma = 1.5$ , as has been done above for the sake of analytical simplicity, introduces, therefore, a quantitative error in the results. It does not, however, affect the validity of the basic conclusion that may be drawn from Eq. (6), namely, that the  $p(t)$  history during combustion is independent of the presence or absence of a balancing chamber, just as in the case, previously treated, of the stationary piston. This result could, of course, have been predicted on the basis of the observation that the volume fraction  $\varphi$  does not appear in Eq. (1).

The entropy rise is again obtained as

$$\Delta S = m_1 \left( c_v \ln \frac{p_f}{p_i} + c_p \ln \frac{v_{f1}}{v_{i1}} \right)$$

In this case,  $p_i$  and  $t_i$  being given,  $p_f$  is calculated from Eq. (6) for  $t = t_i + t_c$ . Then,

$$V_{f2} = V_{i2} \left( \frac{p_i}{p_f} \right)^{1/\gamma}$$

hence,

$$\begin{aligned} V_{f1} &= V_{ft} - V_{i2} \left( \frac{p_i}{p_f} \right)^{1/\gamma} \\ &= V_{it} \left[ \frac{V_{ft}}{V_{it}} - \varphi \left( \frac{p_i}{p_f} \right)^{1/\gamma} \right] \end{aligned}$$

$$\frac{v_{f1}}{v_{i1}} = \frac{V_{f1}}{V_{i1}} = \frac{\frac{V_{ft}}{V_{it}} - \varphi \left( \frac{p_i}{p_f} \right)^{1/\gamma}}{1 - \varphi}$$



Therefore,

$$\Delta S \sim (1-\varphi) \ln \left[ \frac{V_{tf} \left( \frac{P_i}{P_f} \right)^{\frac{1}{\gamma}}}{V_{ti} (1-\varphi)} \right] \quad (7)$$

Now,  $\frac{V_{tf}}{V_{ti}} \left( \frac{P_i}{P_f} \right)^{\frac{1}{\gamma}}$  is always greater than 1.0\*. Therefore, the

antilogarithm in Eq. (7) is always greater than 1.0, and it follows, as in the case of the stationary piston, that the proposed utilization of pressure exchange has the effect of increasing the available work for any given energy input.

\* It would be 1.0 only if the entire process, in both chambers 1 and 2, were isentropic.

## APPENDIX-2

### Derivation of Equations and Sample Calculations:—

#### Nomenclature:—

a	Speed of Sound (dimensional)
A	Speed of Sound (Nondimensional)
H	Heat Input per unit weight of Fuel
J	Mechanical Equivalent of Heat
K; $K_1$	Constants
M	Mach Number
p	Pressure
P, Q	Riemann Variables
Q	Heat released in the Combustion process
S	Entropy (Nondimensional)
T	Temperature
u, v	Velocity (dimensional)
U, V	Velocity (Nondimensional)
$\gamma$	Specific Heat Ratio
$\alpha$	Cross-Sectional Area; Air-Fuel Ratio

#### Subscripts

b	Burned Condition
c	Combustion
f	Flame
o	Initial
s	Shock
u	Unburned Condition

### Definition of Riemann Variables:-

The Riemann Variables are defined by the following equations:

$$P = \frac{2}{\gamma-1} A + U \quad - (a)$$

$$Q = \frac{2}{\gamma-1} A - U \quad - (b)$$

For  $\gamma = 1.4$  we then have

$$P = 5 A + U \quad - (c)$$

$$Q = 5 A - U \quad - (d)$$

From (c) and (d) we get

$$U = \frac{P-Q}{2}$$

$$\text{and } A = \frac{P+Q}{10}$$

### Nonsteady Flow Analysis of NAHB Combustion Process:-

#### Derivation of Equations and Sample Calculations:

Consider the flame propagation in a constant area duct as shown in figure (1) below.

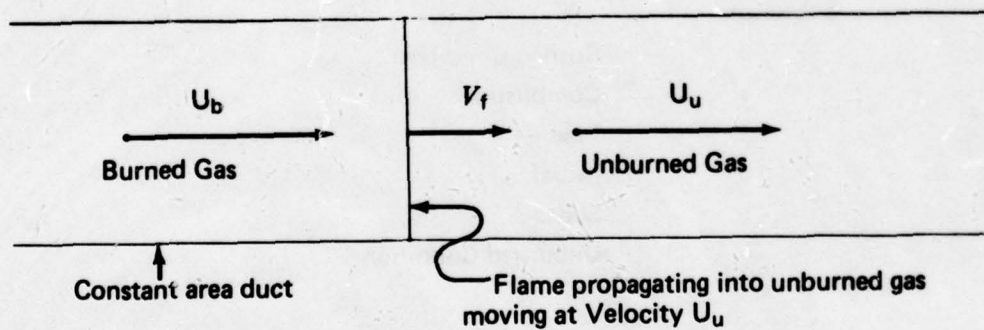


Fig. 1. Flame propagation in a constant area duct.

From the conservation of mass and energy and from the equation of state the following equation can be derived.

$$U_b = U_u - V_f \left[ \frac{\gamma_b - 1}{\gamma_b} \frac{\gamma_u}{\gamma_u - 1} \left( 1 + \frac{K_1}{A_u^2} \right) - 1 \right] \quad - (1)$$

Equation VI. h. 8 of reference (3)

where

$$K_1 = (\gamma_u - 1) g J Q / a_o^2$$

For the case of constant specific heats on both sides of the flame front we have

$$\gamma_u = \gamma_b$$

and equation (1) reduces to

$$U_b = U_u - V_f \frac{K_1}{A_u^2} \quad (2)$$

Furthermore, assuming that the burning velocity,  $v_f$  is proportional to the temperature of the unburned gas,

$$v_f = K T_u = K \frac{a_u^2}{\gamma_u R g} \quad (3)$$

$$V_f = \frac{v_f}{a_o} = K \frac{a_o A_u^2}{\gamma R g} \quad (4)$$

Substituting equation (4) into equation (2) we get

$$U_b = U_u - \frac{K Q}{c_p a_o} = \frac{K H \eta_c}{c_p a_o (\alpha + 1)} \quad (5)$$

However, since the burned gas is adjacent to a closed end of the duct, we have

$$U_b = 0$$

and from equation (5), 
$$U_u = \frac{K Q}{c_p a_o} = \frac{K H \eta_c}{c_p a_o (\alpha + 1)} \quad (6)$$

where

$$\begin{aligned} Q &= \text{Heat Input per unit weight of fuel.} \\ &= \frac{H \eta_c}{(\alpha + 1)} \end{aligned}$$

Let the initial conditions of the gas in the duct be such that:

$$H = \text{Heating value of fuel} = 19,000 \frac{\text{Btu}}{\text{lb}}$$

$$\alpha = \text{Air-Fuel ratio} = 20$$

$$v_f = 100 \frac{\text{ft}}{\text{sec}} @ T = 540^\circ \text{R}$$

$$\eta_c = \text{combustion efficiency} = 90\%$$

$$T_o = \text{Initial temperature of air} = 1200^\circ \text{R}$$

$$a_o = \text{Initial speed of sound} = 1700 \frac{\text{ft}}{\text{sec}}$$

$$\text{Then } v_f = 222.22 \frac{\text{ft}}{\text{sec}} @ 1200^\circ \text{R}$$

$$K = \frac{100}{540} = 0.185$$

From equation (6),  $U_u = 0.370$

The gas ahead of the flame front is accelerated from rest to this velocity.

The strength of the Initial Shock is given by

$$\frac{|\Delta u|}{A} = \frac{U_u - U_o}{A_o} = \underline{0.370}$$

Then we have from shock tables 1 a of reference (3)

$$\frac{A'}{A} = A_u = 1.076 ; \frac{p'}{p} = 1.65$$

$$M_s = 1.247 \leftarrow \text{Shock Mach Number}$$

$$\Delta S = S_u - S_o = 0.009$$

$$V_f = \frac{V_f}{a_o} = \frac{222.22}{1700} = 0.13$$

$$\begin{aligned} W_f &= \text{Velocity of flame front relative to the duct} \\ &= U_u + V_f = 0.37 + 0.13 = 0.50 \end{aligned}$$

$$\text{Also, } K_1 = \frac{(\gamma - 1) g J Q}{a_o^2} = 2.8234$$

$$A_b = A_u \left( 1 + \frac{K_1}{A_u^2} \right)^{1/2} = 1.995$$

$$\begin{aligned} S_b &= S_u + \frac{2}{\gamma - 1} \ln \left( \frac{A_b}{A_u} \right) \\ &= 0.009 + 5 \ln \left( \frac{1.995}{1.076} \right) = 3.096 \end{aligned}$$

Thus for the above interaction, the numerical results obtained are shown in Figure (2) Below.

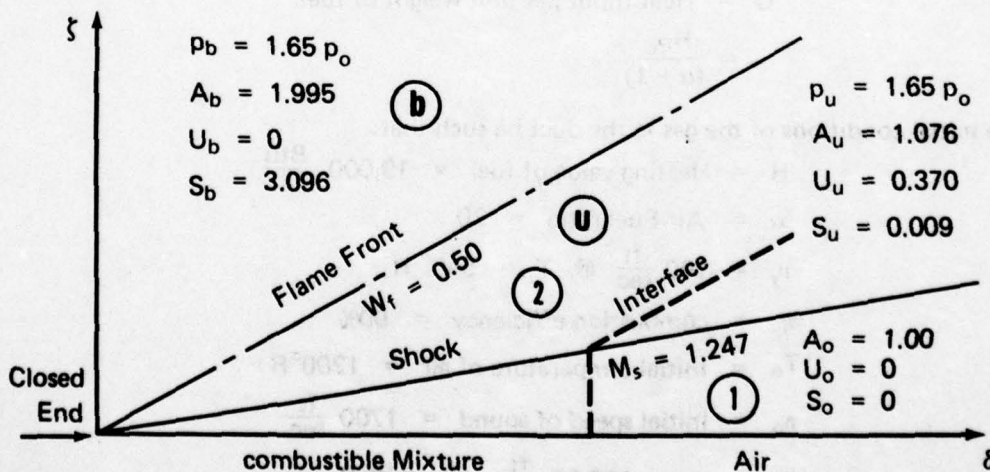
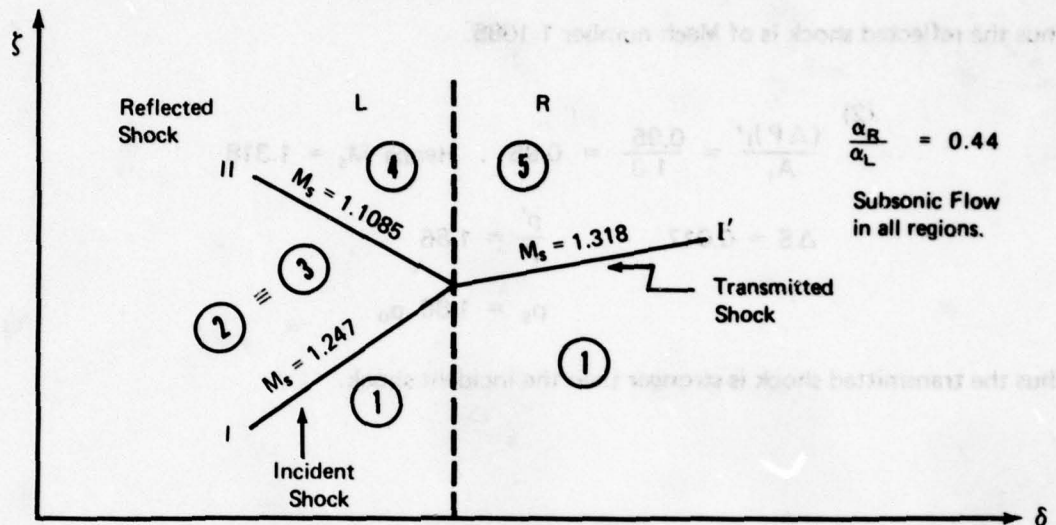


Fig. 2. Flame Front advancing into a combustible mixture.  
(Ignition at a closed end of the duct)

**Interaction of the Initial Shock ( $M_s = 1.247$ ) at the first change of cross-section:—**

Let subscripts L and R denote conditions immediately to the left and to the right, respectively, of a discontinuous area change. Assuming that the flow is subsonic on both sides, the step section is reached by an p characteristics from the left and by a Q characteristics from the right. Therefore,  $P_L$  and  $Q_R$  are known.



**Fig. 3. Shock at a discontinuous change of cross-section.**

Since the shock is weak,  $P_4 = P_3 = 5.75$   
and  $Q_5 = Q_1 = 5.0$

Then for regions (4) and (5)

$$\frac{P_L}{Q_R} = \frac{P_4}{Q_5} = \frac{5.75}{5.0} = 1.15 \quad \text{and} \quad \frac{\alpha_R}{\alpha_L} = 0.44$$

With the above known values go to figure

6 e - 4 (FOA). We then have

$$\frac{Q_L}{P_L} = \frac{Q_4}{P_4} = 0.934 \Rightarrow Q_4 = 5.3705$$

$$\text{and} \quad \frac{P_R}{Q_R} = \frac{P_5}{Q_5} = 1.19 \Rightarrow P_5 = 5.95$$

$$A_4 = \frac{P_4 + Q_4}{10} = 1.112 \quad U_4 = \frac{P_4 - Q_4}{2} = 0.19$$

$$(1) \frac{(\Delta Q)_{II}}{A_3} = \frac{0.3705}{1.076} = 0.344. \text{ Hence } M_{s_{II}} = 1.1085$$

$$\Delta S = 0.001 \quad \frac{p'}{p} = 1.265$$

$$p_3 = 1.65 p_0 \quad p_4 = 1.265 (1.65 p_0) \\ = 2.08725 p_0$$

Thus the reflected shock is of Mach number 1.1085.

$$(2) \frac{(\Delta P)_{I'}}{A_1} = \frac{0.95}{1.0} = 0.95. \text{ Hence } M_s = 1.318$$

$$\Delta S = 0.017 \quad \frac{p'}{p} = 1.86$$

$$p_5 = 1.86 p_0$$

Thus the transmitted shock is stronger than the incident shock.

The above computations are summarized below in tabular form.

$$P = \frac{2}{\gamma - 1} A - u \quad A = \frac{P + Q}{10}$$

$$Q = \frac{2}{\gamma - 1} A - u \quad U = \frac{P - Q}{2}$$

Region	p	Q	U	A	S	p'/p <sub>0</sub>
1	5	5	0	1	0	1.00
2	5.75	5	0.37	1.076	0.009	1.65
3	5.75	5	0.37	1.076	0.009	1.65
4	5.75	5.3705	0.19	1.112	0.01	2.08725
5	5.95	5.0	0.475	1.095	0.017	1.86

Following the method described above, the nature of the subsequent interactions of the transmitted shock ( $M_s = 1.318$ ) and the resulting transients at downstream discontinuous change of cross-sections can be determined. The details of the computations are given below.

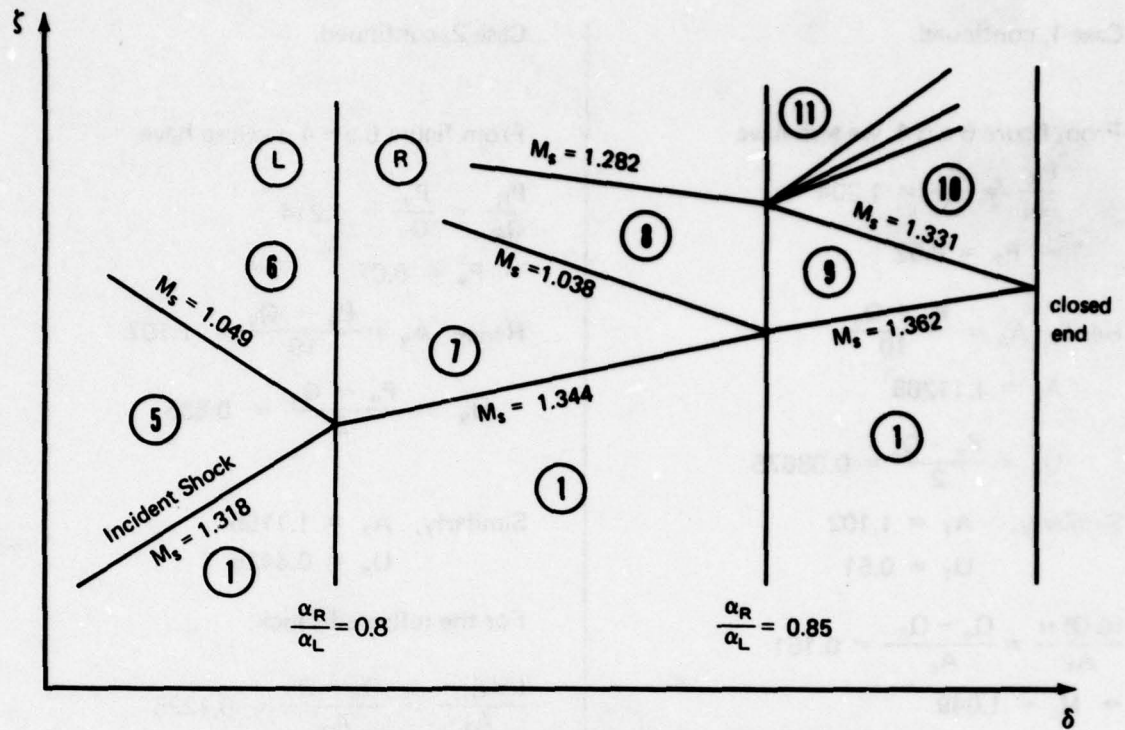


Fig. 4. Shock at discontinuous change of cross-section.

Case 1.

$$\frac{\alpha_R}{\alpha_L} = 0.8$$

Since the incident shock is weak,

$$P_6 = P_5 = 5.95$$

and  $Q_7 = Q_1 = 5.0$

Then for regions (6) and (7)

$$\frac{P_L}{Q_R} = \frac{P_6}{Q_7} = 1.19 \text{ and } \frac{\gamma_R}{\gamma_L} = 0.8$$

With the above known values to figure  $6e-4$  (FOA).

Then from figure

$$\frac{Q_L}{P_L} = \frac{Q_6}{P_6} = 0.870$$

$$\Rightarrow Q_6 = 5.1765$$

Case 2.

$$\frac{\alpha_R}{\alpha_L} = 0.85$$

Since the incident shock is weak,

$$P_8 = P_7 = 6.02$$

and  $Q_9 = Q_1 = 5.0$

Then for regions (8) and (9)

$$\frac{P_L}{Q_R} = \frac{P_8}{Q_9} = 1.204$$

With the above known values from figure  $6e-4$

$$\frac{Q_L}{P_L} = \frac{Q_8}{P_8} = 0.853$$

$$\Rightarrow Q_8 = 5.135$$



Case 1, continued.

From figure 6 e - 4 we also have

$$\frac{P_R}{Q_R} = \frac{P_7}{Q_7} = 1.204$$

$$\Rightarrow P_7 = 6.02$$

$$\text{Hence } A_6 = \frac{P_6 + Q_6}{10}$$

$$A_6 = 1.11265$$

$$U_6 = \frac{P_6 - Q_6}{2} = 0.38675$$

$$\text{Similarly, } A_7 = 1.102$$

$$U_7 = 0.51$$

$$\frac{(\Delta Q)_\Pi}{A_5} = \frac{Q_6 - Q_5}{A_5} = 0.161$$

$$\Rightarrow M_5 = 1.049$$

$$\frac{p'}{p} = 1.12 \text{ from shock table.}$$

$$\text{Thus } p_6 = 1.12 p_5$$

$$\frac{\Delta u}{A_5} = 0.08$$

$$U_5 - U_6 = 0.0876$$

Thus the Reflected Shock is of Mach number 1.049.

---

For the transmitted shock,

$$\frac{(\Delta P)_{I'}}{A_1} = \frac{P_7 - P_1}{A_1} = 1.02$$

$$\Rightarrow (M_5)_{I'} = 1.344$$

$$\frac{p'}{p} = 1.94 \Rightarrow p_7 = 1.94 p_1$$

Case 2, continued.

From figure 6 e - 4 we also have

$$\frac{P_R}{Q_R} = \frac{P_9}{Q_7} = 1.214$$

$$\Rightarrow P_9 = 6.07$$

$$\text{Hence } A_9 = \frac{P_9 + Q_9}{10} = 1.107$$

$$U_9 = \frac{P_9 - Q_9}{2} = 0.535$$

$$\text{Similarly, } A_8 = 1.1155$$

$$U_8 = 0.4425$$

For the reflected shock,

$$\frac{(\Delta Q)_\Pi}{A_7} = \frac{Q_8 - Q_7}{A_7} = 0.1225$$

$$\Rightarrow M_5 = 1.03775$$

$$\frac{p'}{p} = 1.09$$

$$\text{Hence } p_8 = 1.09 p_7$$

Thus the reflected shock is of Mach number 1.038.

---

For the transmitted shock,

$$\frac{(\Delta P)_{I'}}{A_1} = \frac{P_9 - P_1}{A_1} = 1.07$$

$$\Rightarrow (M_5)_{I'} = 1.362$$

$$\frac{p'}{p} = 2.0 \Rightarrow p_9 = 2p_1$$

Shock @ closed end: -

$$\text{Strength of reflected shock} = \frac{|\Delta u|}{A} = \frac{u_9}{A_9}$$

$$= \frac{0.535}{1.107} = 0.483 \text{ and } U_{10} = 0$$

$$\Rightarrow M_s = 1.331 \quad \frac{p'}{p} = 1.905$$

$$\frac{A'}{A} = 1.1005 \Rightarrow A_{10} = 1.21825. \quad p_9 = 2 p_0$$

$$\Delta S = 0.0195 \text{ and } Q_{10} = P_{10} = 5 A_{10} = 6.09$$

$$p_{10} = 1.905 (p_9) = 3.81 p_0$$

Reflected shock at change of cross-section.

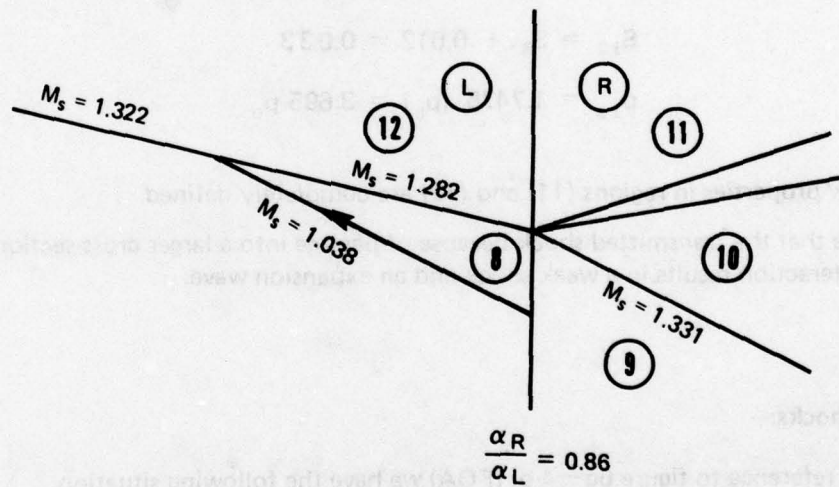


Fig. 5. Shock at change of cross-section.

$$\left. \begin{array}{l} Q_{10} = Q_{11} = 6.09 \\ P_8 = P_{11} = 6.02 \end{array} \right\} \frac{P_L}{Q_R} = \frac{P_{12}}{Q_{11}} = \frac{6.02}{6.09} = 0.9885$$

$$\text{From figure 6 e-7 ; } \frac{P_R}{Q_R} = \frac{P_{11}}{Q_{11}} = 0.99 \Rightarrow P_{11} = 6.029$$

$$\frac{Q_L}{P_L} = \frac{Q_{12}}{P_{12}} = 1.01 \Rightarrow Q_{12} = 6.0802$$

$$\frac{Q_{12} - Q_8}{A_8} = 0.8473 \rightarrow M_s = 1.282 \quad \Delta S = .012$$

$$\frac{p'}{p} = 1.7475$$

$$\frac{P_{11} - P_{10}}{A_{10}} = \frac{6.029 - 6.09}{1.21825} \rightarrow \text{EXPN WAVE}$$

$$U_{11} = (P_{11} + Q_{11})/2 = -0.0305$$

Hence the flow in region (11) has a negative velocity.

$$A_{11} = \frac{(P_{11} - Q_{11})}{10} = 1.212$$

Similarly for region 12, we have

$$P_{12} = 6.02 \text{ and } Q_{12} = 6.0802$$

$$\text{Hence } U_{12} = -0.0301 \text{ and } A_{12} = 1.210$$

$$S_{12} = S_8 + 0.012 = 0.033$$

$$p_{12} = 1.7475 (p_8) = 3.695 p_0$$

Thus all flow properties in regions (11) and (12) are completely defined.

Note that the transmitted shock because of passage into a larger cross-sectional area. Thus this interaction results in a weak shock and an expansion wave.

#### Merging of shocks:—

With reference to figure 6g - 4 of (FOA) we have the following situation.

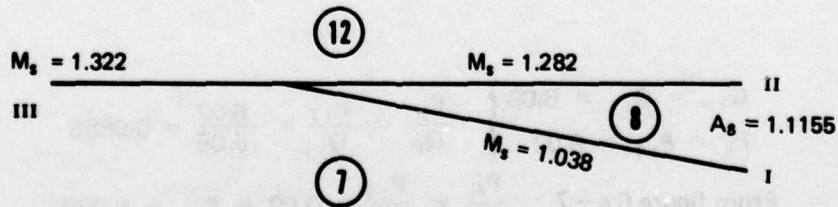


Fig. 6. Merging of Weak Shocks

For the case of weak shocks, we have

$$(\Delta A)_{III} = (\Delta A)_I + (\Delta A)_{II} = 0.108$$

$$\text{Since } (\Delta A)_I = A_8 - A_7 = 0.0135$$

$$\text{and } (\Delta A)_{II} = A_{12} - A_8 = 0.0945$$

Then we get

$$(\Delta A)_{III} = A_{12} - A_7 = 0.108$$

$$\frac{A_{12}}{A_7} = 1 + \frac{0.108}{1.102} = 1.098$$

Now from shock tables we have  $\frac{p'}{p} = 1.87$  and

$$M_s = 1.322 \text{ propagating into region 7 .}$$

$$A_{12} = 1.098 A_7 = 1.210.$$

It can be seen that the merger produces a stronger shock.

#### Interaction of Flame Front with the First Reflected Shock:

Figure (7) below shows a typical interaction involving a flame front and a shock wave. The matching condition across the flame front are the pressure and flow velocity.

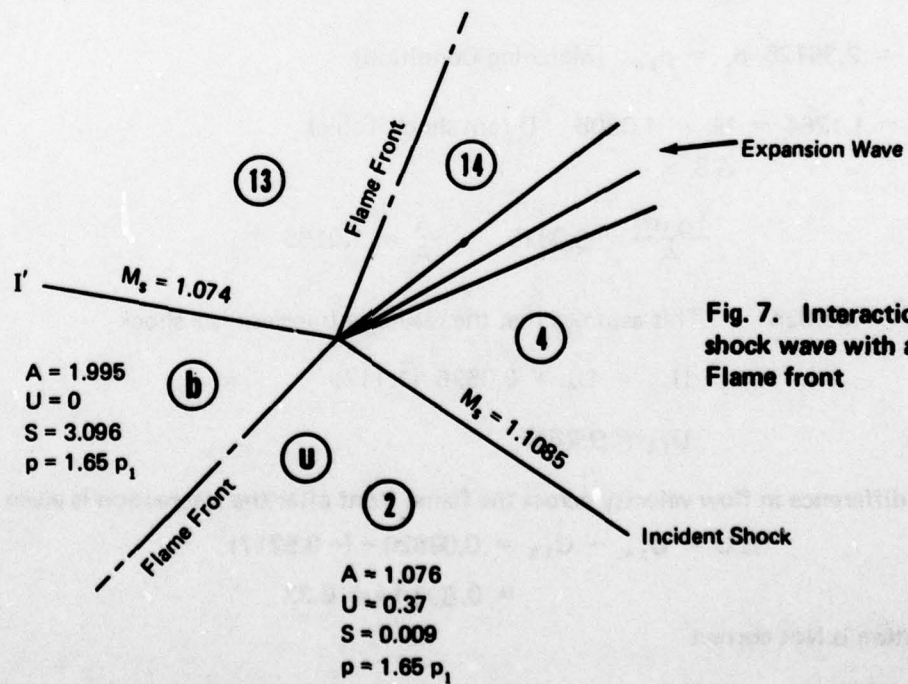


Fig. 7. Interaction of shock wave with a Flame front

Guess  $A_{13} = 2.1$

$$\text{Then } \frac{A_{13}}{A_6} = \frac{2.1}{1.995} = 1.0526$$

Now from shock tables we have

$$M_s = 1.1685 \quad \frac{p'}{p} = 1.425$$

$$\frac{|\Delta u|}{A_b} = 0.2615 \quad \Delta S = .0035 \text{ etc.}$$

$$U_{13} = -0.5217$$

Note:—

For a Q shock

$$\frac{|\Delta u|}{A} \Rightarrow \frac{U_{\text{ahead}} - U_{\text{behind}}}{A_{\text{ahead}}}$$

$$\text{Hence } 0.2615 = \frac{U_b - U_{13}}{A_b}$$

and since  $U_b = 0$  (Velocity adjacent to the closed wall)

$$U_{13} = -0.2615 (1.995) = -0.5217 \leftarrow$$

---

$$\text{Also } \frac{p_{13}}{p_1} = [1.425 (1.650)] = 2.35125$$

Hence  $p_{13} = 2.35125 p_1 = p_{14}$  [Matching Condition]

$$\text{When } \frac{p_{14}}{p_4} = 1.1264 \Rightarrow M_s = 1.0505 \quad (\text{From shock Table})$$

$$\Delta S = 0$$

$$\frac{|\Delta u|}{A} = 0.0825 \quad \frac{A'}{A} = 1.0165$$

$$\frac{U_{14} - U_4}{A_4} = 0.0825$$

This assumes that the resulting transient is a shock

$$U_{14} = U_4 + 0.0825 (1.112)$$

$$U_{14} = 0.2817$$

Hence the difference in flow velocity across the flame front after the interaction is given by

$$\begin{aligned} \Delta U &= U_{14} - U_{13} = 0.09826 - (-0.5217) \\ &= 0.80344 \neq 0.37 \end{aligned}$$

Hence solution is Not correct

2nd Trial (Identical to the procedure describe above)

Guess  $A_{1,3} = 2.0425$

Then  $\frac{A_{1,3}}{A_b} = 1.0238$

From shock table, we have the following:—

$$M_5 = 1.074 \quad \Delta S = 0 \quad \frac{p'}{p} = 1.18$$

$$\frac{|\Delta U|}{A} = 0.120 = \frac{U_b - U_{1,3}}{A_b} \quad U_b = 0$$

$$U_b - U_{1,3} = 0.2394 \Rightarrow U_{1,3} = -0.2394$$

$$p_{1,3} = 1.947 \quad p_1 = p_{1,4} \quad \text{[Matching condition]}$$

$$\frac{p_{1,4}}{p_4} = 0.9328 = \left(\frac{A_{1,4}}{A_4}\right)^7 \quad \text{For Isentropic Waves since } p_{1,4} < p_4$$

Thus the resulting transient is an expansion Wave. And for a P – expansion Wave

$$Q_{1,4} = Q_4 = 5.3705$$

$$\begin{aligned} \frac{A_{1,4}}{A_4} = 0.990 &\Rightarrow A_{1,4} = 1.101 \\ U_{1,4} = 5 A_{1,4} - Q_{1,4} \\ U_{1,4} &= 0.1345 \end{aligned}$$

$$\Delta U = U_{1,4} - U_{1,3} = 0.1345 + 0.2394 = 0.3739$$

Velocity ↑  
ahead of  
flame-front

↑ Velocity behind  
the flame-front

Hence  $\Delta u] = 0.37 \cong 0.3739 = \Delta U] \leftarrow$  Matching  
before condition  
interaction After  
Interaction

Thus the trial solution is Correct

**Shock at closed End:—**

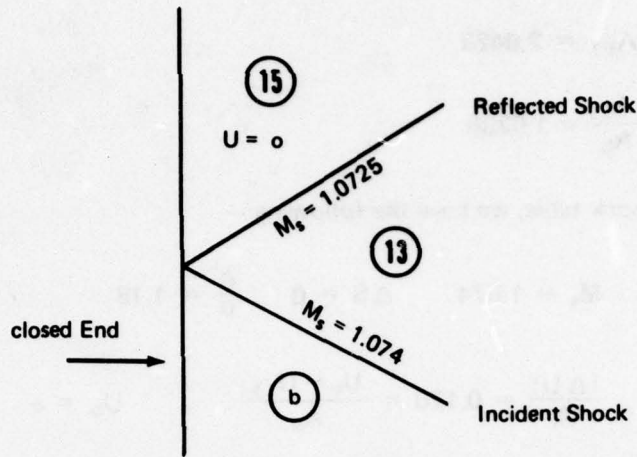


**Fig. 8. Shock Reflection at closed end**

Since  $U_{15} = 0$  (Region adjacent to the closed end)

$$\frac{|\Delta u|}{A_{13}} = \frac{U_{13}}{A_{13}} = \frac{0.2394}{2.0425} = 0.1172 \Rightarrow M_s = 1.0725$$

$$= \frac{A'}{A} = 1.0235 \quad \text{and} \quad \frac{p'}{p} = 1.175$$

Hence  $A_{15} = 2.0905$      $p_{15} = 2.2877 p_1$

$$\Delta S = 0 \Rightarrow S_{15} = S_{13} = 3.096$$

The Reimann parameters are determined as follows:—

$$P_{15} = 5 A_{15} + U_{15} = 10.4525$$

$$Q_{15} = 5 A_{15} - U_{15} = 10.4525$$

Interaction of shock and Flame Front:-

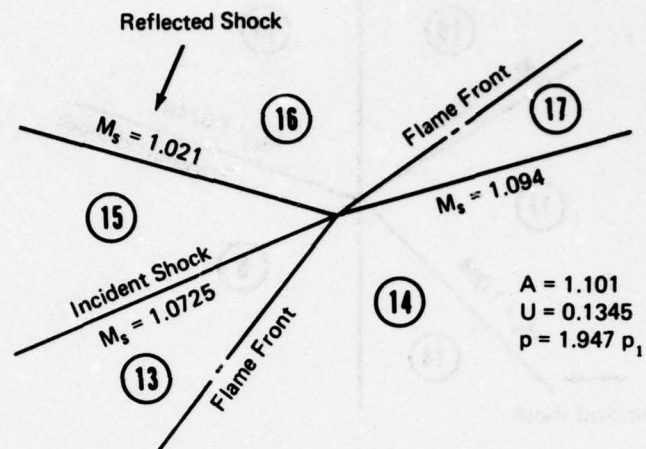


Fig. 9. Shock-Flame Front Interaction:-

This interaction is identical to the one shown in figure (7).

Guess  $A_{16} = 2.105$

$$\text{Then } \frac{A_{16}}{A_{15}} = 1.007 \Rightarrow M_s = 1.021 \text{ and } \frac{p'}{p} = 1.05$$

(From shock tables)

$$\frac{|\Delta u|}{A} = 0.035 \Rightarrow \frac{U_{15} - U_{16}}{A_{15}} = 0.035$$

$$U_{16} = -0.073$$

$$p_{16} = 1.05 p_{15} = p_{17} \quad (\text{Matching condition})$$

$$\frac{p_{17}}{p_{14}} = 1.2337 \Rightarrow \text{Resulting transient is a shock of } M_s = 1.094 \text{ and}$$

$$\frac{|\Delta U|}{A} = 0.150 \Rightarrow \frac{U_{17} - U_{14}}{A_{14}} = 0.150$$

Hence  $U_{17} = 0.29965$  and  $\Delta U = 0.37265$

$$\frac{A'}{A} = 1.03 \Rightarrow A_{17} = 1.134$$



**Shock at change of cross-section:—**

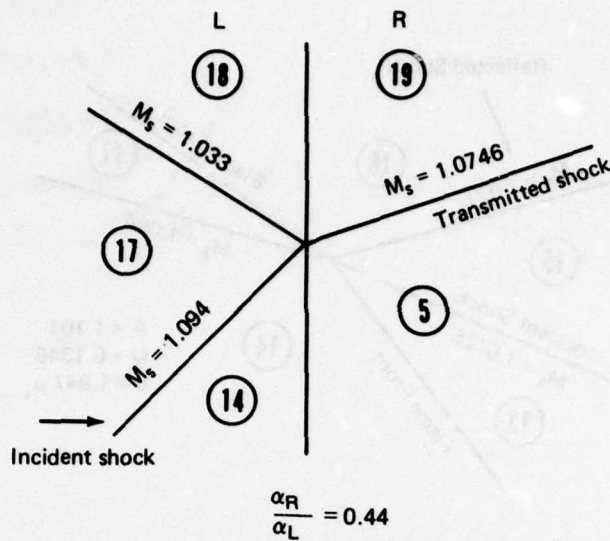


**Fig. 10. Shock at Area-change**

Since the Incident shock is very weak we have

$$P_{17} = P_{18} = 5.97 \text{ and}$$

$$Q_{19} = Q_5 = 5.0$$

Hence  $\frac{P_L}{Q_R} = \frac{P_{18}}{Q_{19}} = \frac{5.97}{5.0} = 1.194.$

With the known value of  $\frac{P_L}{Q_R}$  go to figure 6 e - 4 and obtain

$$\frac{Q_L}{P_L} = \frac{Q_{18}}{P_{18}} = 0.92 \Rightarrow Q_{18} = 5.4924$$

and  $\frac{P_R}{Q_R} = \frac{P_{19}}{Q_{19}} = 1.243 \Rightarrow P_{19} = 6.215$

$$U_{19} = 0.6075 \text{ and } A_{19} = 1.1215$$

$$U_{18} = 0.2388 \text{ and } A_{18} = 1.14624$$

Now for the transmitted shock

$$\frac{(\Delta P)}{A} = \frac{P_{19} - P_5}{A_5} = 0.242 \Rightarrow M_s = 1.0746 \text{ and } \frac{p'}{p} = 1.182$$

And for the reflected shock

$$\frac{(\Delta Q)}{A} = \frac{Q_{18} - Q_{17}}{A_{17}} = 0.1076 \Rightarrow M_s = 1.033 \text{ and } \frac{p'}{p} = 1.075.$$

### Crossing of a contact surface by a shock Wave:—

This type of interaction appears in a wave diagram as shown in figure (11) for a Q - shock crossing an interface

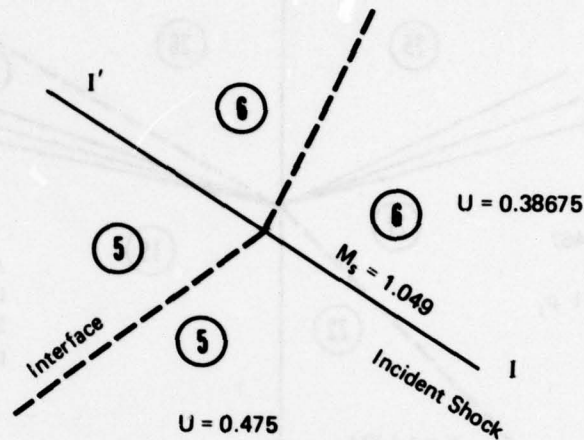
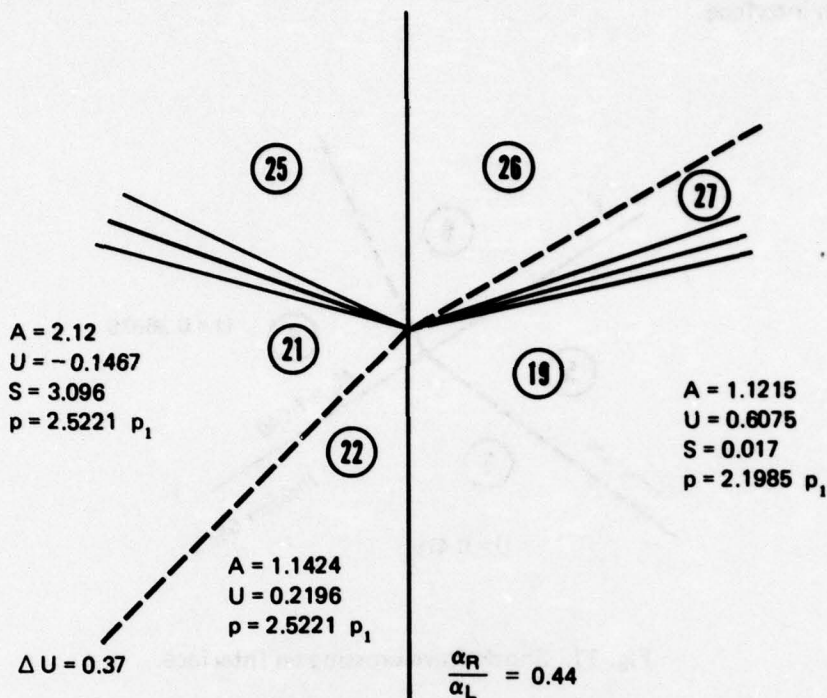


Fig. 11. Shock Wave crossing an Interface.

It is to be noted that for a weak Q - shock I crossing an interface with  $\gamma_R = \gamma_L$ , in general we may expect a transmitted wave I' and a reflected wave II to emerge from the crossing point. However in the present case, the interface which merely separates the combustible mixture of gases from air, is unaffected by the passage of the shock because of the absence of any entropy gradients across the interface. However the interface is slowed down by the incident shock as can be seen by comparing the flow velocities across the interface in regions (5) and (6) respectively.

Thus, we have  $U_5 = 0.475$   
and  $U_6 = 0.38675$ .

**Flame Front at First Change of Cross-section:—**



**Fig. 12. Flame Front @ change of cross-section**

The matching condition across the flame front are the pressure and  $\Delta U$ . Assuming that the resulting transient is an isentropic expansion wave across regions (21) and (25) we have

$$P_{25} = P_{21} = 10.453$$

Now Guess  $A_{25} = 2.075$

Then  $\frac{A_{25}}{A_{21}} = \frac{2.075}{2.12} = 0.9787$

Also we have  $\frac{P_{25}}{P_{21}} = \left(\frac{A_{25}}{A_{21}}\right)^7$  for an isentropic wave

Now  $U_{25} = P_{25} - 5 A_{25} = 0.078$

$$M_{25} = \frac{U_{25}}{A_{25}} = 0.0376$$

We then have  $D_{25} = 0.0376$  (From the table of Mach Number Functions)

Now from the conservation of mass for regions (25) and (26) we get

$$D_{25} \alpha_{25} = D_{26} \alpha_{26}$$

$$D_{26} = D_{25} \frac{\alpha_{25}}{\alpha_{26}} = D_{25} \left( \frac{\alpha_L}{\alpha_R} \right) = \frac{D_{25}}{0.44}$$

$$D_{26} = 0.0852 \Rightarrow M_{26} = 0.0855 \quad (\text{From the table of Mach Number Functions})$$

From the conservation of Energy for regions (25) and (26) we have

$$A_{25}^2 + \frac{\gamma-1}{2} U_{25}^2 = A_{26}^2 + \frac{\gamma-1}{2} U_{26}^2$$

$$\text{or } 5 A_{25}^2 + U_{25}^2 = 5 A_{26}^2 [1 + 0.2 M_{26}^2]$$

$$\text{Hence } 21.5340 = 5.00731 A_{26}^2$$

$$A_{26} = 2.07377$$

$$\text{and } U_{26} = 0.177$$

$$\frac{p_{25}}{p_{21}} = 0.860096 \Rightarrow p_{26} = 2.169 p_1$$

Now for the Isentropic flow regions (25) and (26) we have

$$\frac{p_{26}}{p_{25}} = \left( \frac{A_{26}}{A_{25}} \right)^7 = \left( \frac{2.07377}{2.075} \right)^7 = 0.99585$$

$$p_{26} = 2.169 (0.99585) p_1 = 2.16 p_1$$

$$\text{Hence } p_{27} = p_{26} = 2.16 p_1 \quad (\text{Matching condition})$$

$$\text{Now } \frac{p_{27}}{p_{19}} = 0.9825 \Rightarrow \text{Expansion Wave}$$

$$\frac{A_{27}}{A_{19}} = (0.9825)^{1/\gamma} = 0.99748$$

$$A_{27} = 1.11867$$

$$\text{Also } Q_{27} = Q_{19} = 5.00 \text{ across the expansion Wave}$$

$$U_{27} = 5 A_{27} - Q_{27} = 0.59337$$

$$\Delta U = U_{27} - U_{26} = 0.5934 - 0.177 = \underline{\underline{0.416}}$$

$$\text{Hence } \Delta U] = 0.37 \cong 0.416 = \Delta U]$$

across flame before  
Interaction

across the flame front after  
Interaction

Hence the solutuion is OK

**Interaction of the Flame front with transmitted shock in the balancing chamber:—**

Figure (13) shows the interaction involving the flame front and a transmitted shock of strength given by  $M_s = 1.258$ . The matching condition across the flame front are the pressure and flow velocity.

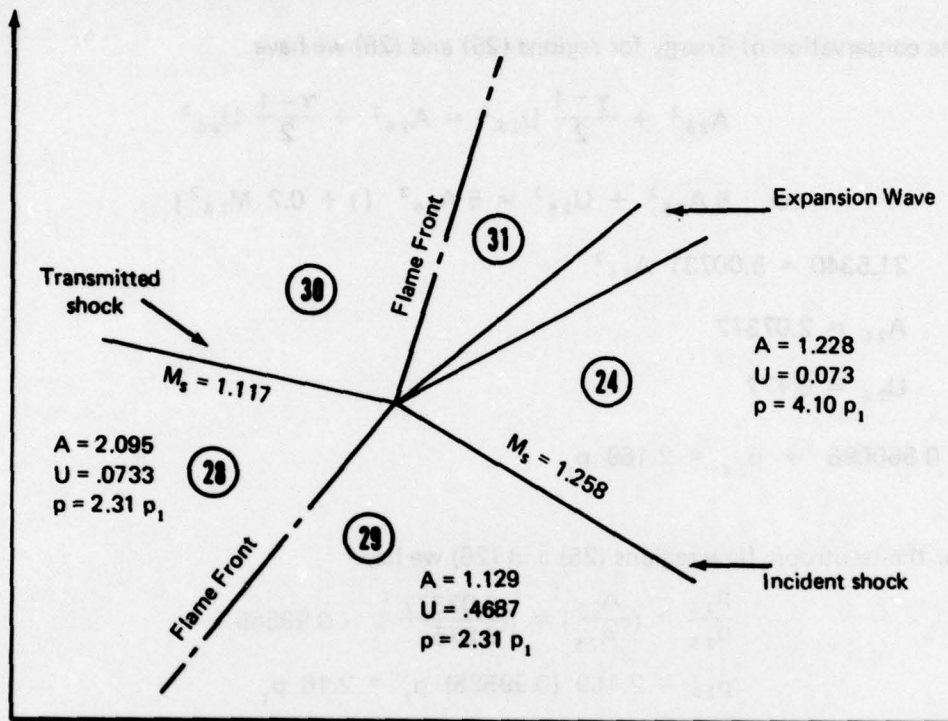


**Fig. 13. Interaction of the shock Wave with a Flame Front:—**

Guess  $A_{30} = 2.21$

Then  $\frac{A_{30}}{A_{28}} = 1.0549$

Now from the shock tables, we have

$$M_s = 1.177 \quad \frac{p'}{p} = 1.45 \quad \Delta S = 0.004$$

$$\frac{|\Delta U|}{A} = 0.273 \quad \text{etc.}$$

For a Q-shock

$$\frac{|\Delta u|}{A} \Rightarrow \frac{U_{\text{ahead}} - U_{\text{behind}}}{A_{\text{ahead}}}$$

Hence  $0.273 = \frac{U_{28} - U_{30}}{A_{28}}$

and thus  $U_{30} = U_{28} - 0.273 (A_{28})$

$$U_{30} = 0.4987$$

Also  $\frac{p_{30}}{p_{28}} = 1.450$

$$p_{30} = 3.3495 p_0 = p_{31} \text{ (Matching condition across the flame front)}$$

Now  $\frac{A_{31}}{A_{24}} = \left(\frac{p_{31}}{p_{24}}\right)^{1/7}$  across an isentropic wave

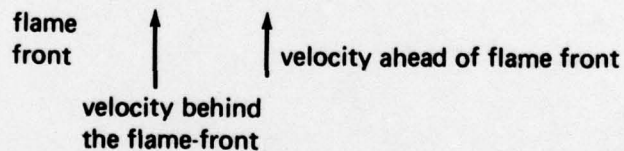
Hence  $\frac{A_{31}}{A_{24}} = \left(\frac{3.3495}{4.10}\right)^{1/7} = 0.9715$

$$A_{31} = 1.193.$$

Now for a P - expansion wave,  $Q_{31} = Q_{24} = 6.069$

$$U_{31} = 5 A_{31} - Q_{31} = -0.1038$$

$$\Delta U] = -U_{30} + U_{31} = 0.395 \leftarrow$$



Hence  $\Delta U]_{\text{before Interaction}} = 0.3954 = 0.395 = \Delta U]_{\text{After Interaction}}$

Thus the matching conditions of pressure and flow velocity across the flame front are satisfied and hence the solution is correct.

It is important to note that the flame front is considerably slowed down as a result of the above interaction and the velocity in region (31) adjacent to the flame front is negative.

**Note:-**

The expansion wave resulting from this interaction is of considerable significance. Thus it is interesting to note that flow velocities in regions (24) and (31) across the expansion wave are of opposite signs. Hence there is a change in flow direction across the expansion wave. The interface also changes direction as a result of this expansion wave and accelerates towards the main combustion chamber and finally reaches the flame front at point A when combustion stops. The interface thus travels towards the main chamber from the balancing chamber as a result of wave interactions.

Thus the slowing down of the flame front and the movement of the interface towards the main chamber is of extreme importance because of the availability of oxygen towards the end of combustion and the increased time available for completion of combustion process in the NAHBE engine.